MATHEMATICAL MODELS OF THE MECHANICS OF THE COCHLEA

Thesis by

Stephen Taylor Neely

In Partial Fulfillment of the Requirements

for the Degree of

Electrical Engineer

California Institute of Technology

Pasadena, California

1978

(Submitted September 6, 1977)

ACKNOWLEDGMENTS

I would like to express my appreciation for the encouragement and guidance of my thesis advisor, Dr. John R. Pierce. I would also like to thank Dr. Jont B. Allen of Bell Laboratories for helping me get started on this research project and my wife, Donna, for helping me get finished. Financial support for this research was provided by the Bell Telephone Laboratories.

ABSTRACT

A two-dimensional mathematical model of cochlear mechanics is developed, based on classical assumptions. The basilar membrane is represented by an acoustic admittance function with longitudinal coupling only through the cochlear fluid. The fluid is assumed to be inviscid and incompressible and all motion in the cochlea is assumed to be linear. The integral equations of Allen (1977) and Siebert (1974) are presented for the infinite cochlea and shown to be Fourier transforms of each other. A two-dimensional finite difference scheme based directly on the model equations is shown to be as accurate as Allen's published solutions and requires only 1/100 the computation time. Numerical solutions are obtained by this direct method for parameters chosen to fit the cochlear map. Traveling-wave solutions are obtained even when the stapes is motionless and the cochlear walls vibrate instead. It is suggested that the initial 9 db/octave slope of the magnitude of the basilar membrane displacement could provide a mechanism for encoding loudness. A new one-dimensional model of the cochlea is proposed which assumes the properties of the basilar membrane to vary slowly along the length of the cochlea. The one-dimensional model provides a link between the two-dimensional model and other one-dimensional, long-wave models.

TABLE OF CONTENTS

1. INTRODUCTION 1

2. BACKGROUND INFORMATION 3

   2.1 Anatomy of the ear 3
   2.2 History of experiments and models 7

3. THE TWO-DIMENSIONAL MATHEMATICAL MODEL 15

   3.1 Cochlear hydrodynamics 18
   3.2 Mathematical formulation 20
   3.3 Summary of model equations 24

4. THE INTEGRAL EQUATIONS FOR THE INFINITE COCHLEA 26

   4.1 Green's function approach 26
   4.2 Fourier transform approach 30
   4.3 Comparison of the integral equations 31

5. FITTING THE EXPERIMENTAL DATA 33

   5.1 Physical dimensions 33
   5.2 The admittance function 33

6. NUMERICAL SOLUTIONS OF THE TWO-DIMENSIONAL MODEL 38

   6.1 Pressure, admittance, and displacement of the basilar membrane 38
   6.2 Variation of model parameters 44

7. THE ONE-DIMENSIONAL MODEL 48

   7.1 The "slowly varying" approximation 48
   7.2 Model equations 50
   7.3 Numerical solutions for displacement of the basilar membrane 51
   7.4 The long-wave approximation 54

8. DISCUSSION OF RESULTS 55

   8.1 Validity of basic assumptions 55
   8.2 Comparison with experiment 57
   8.3 Direct numerical solution 60
   8.4 The "slowly varying" approximation 61
   8.5 Theories of hearing 63

9. SUMMARY AND CONCLUSIONS 65

APPENDIX A. DESCRIPTION OF THE NUMERICAL PROCEDURE FOR THE TWO-DIMENSIONAL FINITE DIFFERENCE SCHEME 68

APPENDIX B. SOLVING THE TRANSCENDENTAL EQUATION BY ITERATION .. 76

REFERENCES 79

LIST OF FIGURES

1. Diagram of the ear 5
2. Cross-section of the cochlear canal 5
3. Results of von Békésy 9
4. Results of Rhode 11
5. Comparison of results of Allen, Zweig et al., and Rhode .. 13
6. Simplified physical model of the cochlea 16
7. Two-dimensional representation of the cochlea 17
8. Velocity source images 28
9. The cochlear map 35
10. Maximum displacement of the partition vs. frequency 35
11. Admittance function vs. distance from the stapes 40
12. Pressure difference vs. distance from the stapes 41
13. Basilar membrane displacement vs. distance from the stapes 42
14. Basilar membrane displacement vs. frequency 43
15. Basilar membrane displacement vs. distance from the stapes with H = 0.05 cm 45
16. Basilar membrane displacement vs. distance from the stapes with upper wall vibrating 46
17. Basilar membrane displacement vs. distance from the stapes with Allen's parameters 47
18. Basilar membrane displacement vs. distance from the stapes with "slowly varying" approximation 53

LIST OF TABLES

I. Comparison of admittance functions 37

II. Sample results of ATNH subroutine 52

III. Comparison of wavelength at the characteristic place 59

1. INTRODUCTION

The cochlea is the inner-ear structure in which mechanical vibrations, representing sound information, are transformed into the neural impulses received by the brain. Evidently, the mechanical structure of the cochlea plays a role in processing the sound signals before they reach the brain. The cochlea is a spiraling tunnel through the temporal bone with a radius of about 1 mm and a length of about 35 mm. Experimental observation of motion within the cochlea is very difficult due to the small amplitudes of vibration and the inaccessibility of the cochlea itself. Hence, there is a need for mechanical and mathematical models to complement our understanding of the function of the cochlea. The purpose of this thesis is to present some new developments in the mathematical modeling of cochlear mechanics. These developments are, basically, 1) a Fourier transform relation between previously published integral equations, 2) a direct numerical procedure for obtaining solutions to a two-dimensional cochlear model, and 3) a one-dimensional model based on a "slowly varying" approximation.

The foundation of this thesis is a simple two-dimensional model of the cochlea. This model is not new, but has evolved through the work of Lien and Cox (1973), Siebert (1974), Lesser and Berkley (1972), and Allen (1977). The model represents the cochlea as a rectangular region filled with an inviscid, incompressible fluid.

Chapter 2 will present a more detailed description of the cochlea and what is known about its function. In chapter 3 the mathematical

equations for the two-dimensional model will be formulated. Chapter 4 presents two integral equations, derived from the model equations, which have been used in an attempt to find solutions to the two-dimensional model. Chapter 5 deals with choosing parameters for the mathematical model which are based on the physical cochlea. Numerical solutions obtained directly from the model equations are presented in chapter 6. A description of the numerical procedure will be found in Appendix A. A one-dimensional model based on the assumption of slowly varying properties within the cochlea is presented in chapter 7. Included in chapter 8 is a discussion of the fidelity of the mathematical modeling and the relation of results obtained to theories and experiments in hearing.

2. BACKGROUND INFORMATION

The central concern of the mathematical models presented in this thesis is a description of the basilar membrane motion within the human cochlea. The purpose of this chapter is to provide a proper context for the remainder of the thesis: first, a brief description of the anatomy and function of the ear with emphasis on the structure of the cochlea (Wever and Lawrence, 1954), and second, a survey of some relevant hearing research.

2.1 Anatomy of the ear

The anatomy of the ear is usually divided into three regions: the outer ear, the middle ear, and the inner ear. The outer ear consists of the pinna and the external auditory meatus. The pinna is the expanded flap of skin on the side of the head which is commonly referred to as the ear. The meatus is a short curved tube about 2.5 cm in length which leads inward from the pinna to the eardrum. The middle ear apparatus lies in an air-filled cavity, the tympanic cavity, just beyond the eardrum in the mastoid portion of the temporal bone. The vibrations of the eardrum are transmitted through the middle ear by means of three small bones: the malleus, the incus, and the stapes. A passageway from the middle ear to the pharynx, called the Eustachian tube, allows the air pressure to be equalized across the eardrum. Finally, the inner ear consists of the cochlea, the vestibule, and the semicircular canals which lie in the bony labyrinth deeper in the petrous part of the

temporal bone. Of these, only the cochlea is concerned with hearing. The other parts of the inner ear serve the sense of spatial orientation. The principal parts of the ear are shown in Fig. 1.

The cochlea is the primary receptor organ for hearing. It is coiled like a snail shell in a flat spiral of two and a half turns. The cochlear chamber is divided into an upper duct and lower duct partly by a thin bony shelf called the spiral lamina and partly by the cochlear partition. The partition stretches across from the spiral lamina to the spiral ligament which attaches it to the outer wall. The upper duct is called the scala vestibuli, because it is nearer the vestibule. The lower duct is called the scala tympani, because it is nearer the tympanic cavity. The cochlear partition is itself a duct, the scala media, bounded by the stiff gelatinous basilar membrane on one side and the more compliant Reissner's membrane on the other. A cross-section of the cochlea which shows the three scalae appears in Fig. 2.

The scala vestibuli and scala tympani contain a liquid called perilymph. They communicate with one another through an opening called the helicotrema, which is located at the apical end of the cochlea. The partition is filled with a different liquid, the endolymph, which provides nutrients to the sensory cells.

At the basal end of the cochlea, the scala vestibuli communicates with the vestibule. Located in the outer wall of the vestibule is the oval window, which is covered by the footplate of the stapes. A corresponding opening in the bony outer wall of the scala tympani, the round window, is covered simply by a thin membrane.

The basilar membrane and bony shelf both terminate at the helico-

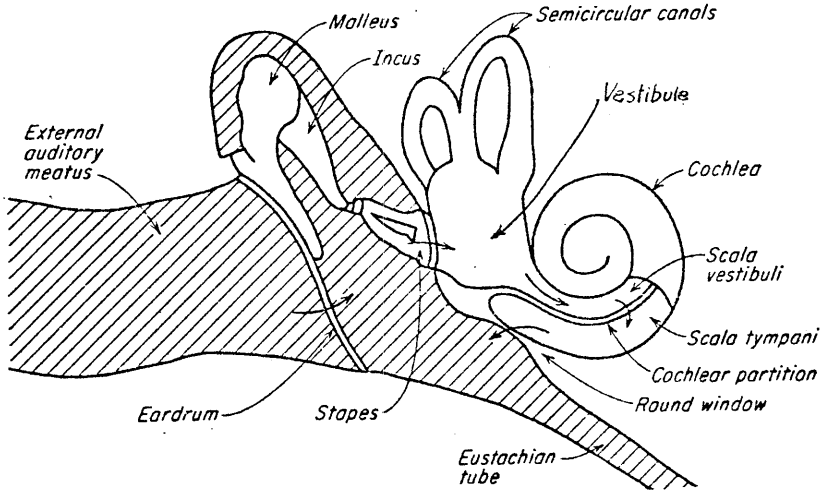

Figure 1. A sectional diagram of the ear, from von Békésy (1960). The arrows indicate the paths of sound.

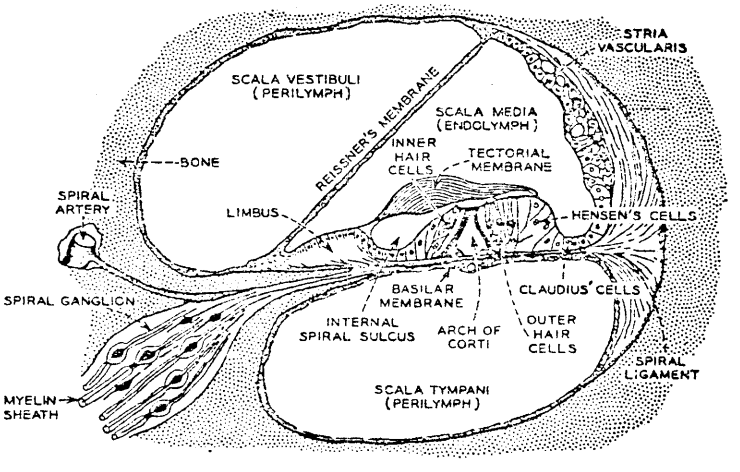

Figure 2. Schematic cross-section of the cochlear canal, from Flanagan (1972).

trema. The basilar membrane is about 35 mm in length and tapers from a width of about 0.08 mm at the base to about 0.5 mm at the apex. The area of the helicotrema is about 0.15 sq. mm.

The process of hearing begins with an acoustic signal in the vicinity of the ear which propagates through the air as a wave of alternating compression and rarefraction. The variation of air pressure in the external auditory meatus sets the eardrum in vibration. These vibrations are transmitted through the malleus and the incus to the footplate of the stapes and produce a displacement of the fluid in the region of the footplate. Very slow vibrations of the stapes result in a to-and-fro movement of fluid between the scala vestibuli and the scala tympani through the opening at the helicotrema. Higher frequency vibrations are transmitted through the yielding cochlear partition. In either case, the volume displacement at the round window is equal to that initiated by the stapedial footplate (von Békésy, 1960).

Within the cochlear partition and lying on the basilar membrane is the organ of Corti containing the final receptor cells, the hair cells. These cells are innervated by nerve fibers that originate in the spiral ganglion a little distance toward the axis of the cochlear spiral. The motion of the cochlear partition stimulates the hair cells by means of the cilia, or tufts of hair, growing on each hair cell. These hairs, at least those of the outer hair cells, are believed to be attached to the tectorial membrane (see Fig. 2). The relative motion between the basilar membrane and the tectorial membrane will bend these tiny hairs causing an electrical pulse to be sent to the brain via one of the 30,000 nerve fibers which innervate the cochlea (Schroeder, 1975).

There is an abundance of data on the nerve firings recorded in single nerve fibers of the auditory nerve. The transformation from basilar membrane motion to neural firing is unknown.

2.2 History of experiments and models

The early Greeks, in the fifth century B.C., conceived of sounds much as we do today, as vibratory movements through the air. They were aware that hearing is the result of the passage of these vibrations into the ear, but had little understanding of the hearing process. Little progress was made in the theory of action of sound until the sixteenth century A.D., when the great anatomists of that age brought to light many hidden parts of the ear. Our modern conception of the anatomy of the ear is a product of many centuries of inquiry (Wever and Lawrence, 1954).

Helmholtz (1954) did considerable physiological work on the anatomy of the ear. Based on his observations, Helmholtz proposed a resonance theory of hearing which first appeared in 1863. The Helmholtz resonance theory considers the cochlear partition as a series of tuned resonators with high tones located at the base and low tones at the apex. In response to a single tone, the cochlear partition would vibrate only in the restricted region which resonates with that particular tone. The analogy is that of a piano, with damper raised, whose strings will vibrate selectively in response to single acoustic tones. This resonance theory had to be revised with the advent of von Békésy's observations of motion of the cochlear partition.

Much of what we know about the functioning of the ear is due to experimental studies of G. von Békésy. von Békésy's observations of

human cadavers, animals, and models began in 1928 and earned him a Nobel prize in 1961. von Békésy devised a technique for measuring the displacement of the cochlear partition in response to a sinusoidal tone. He observed cochleas from animals and fresh human cadavers under a microscope with stroboscopic illumination. Fig. 3 shows a sample of von Békésy's experimental results from a human cochlea. von Békésy was able to observe traveling waves on the basilar membrane; waves that travel up the cochlea with progressively shorter wavelengths and increasing amplitude. These waves reach a maximum at some positions and then fall away rapidly. The location of the displacement maximum or characteristic place, varies with frequency as in the resonance theory. High frequencies travel only a short distance on the basilar membrane, while low frequencies travel further toward the helicotrema. von Békésy observed that, at least at low frequencies, Reissner's membrane vibrates in phase with the basilar membrane, that is, the whole scala media vibrates as a single partition. He also found curious vortex movements of the cochlear fluid in the vicinity of the maximum amplitude. He believed that these eddies also played a significant role in the excitation of the hair cells. von Békésy's experimental results provided a substantial challenge to those who would try to explain the behavior of the cochlea with mathematical models.

Peterson and Bogert (1950) derived a long-wave model based on von Békésy's observations. They assumed that waves propagated in the cochlea were long compared to the cross-sectional diameter and made an analogy to waves on an electrical transmission line. They determined the stiffness of the basilar membrane from von Békésy's test-hair measurements

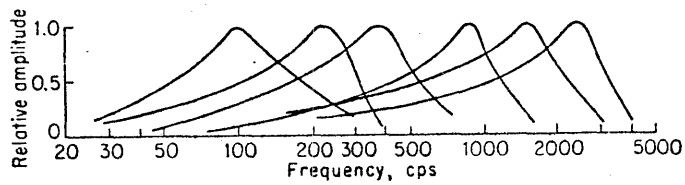

(a)

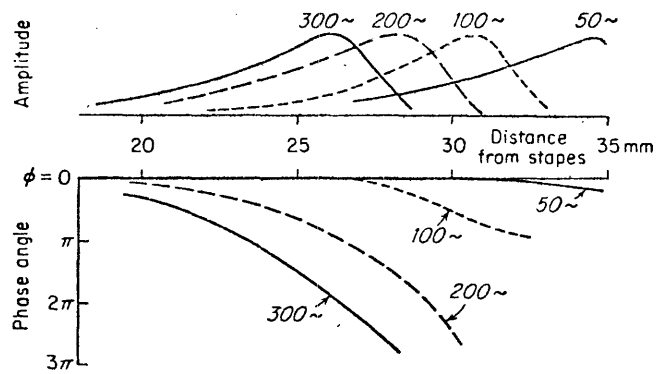

(b)

Figure 3. Results of von Békésy's observation of the vibration of the cochlear partition in human cadavers. (a) Relative amplitude of the displacement versus frequency for six positions along the cochlea. (b) Relative amplitude and phase of the basilar membrane displacement for four low frequencies. From von Békésy (1960).

and used the fluid mass inside the cochlear duct as the partition mass. They assumed elements of the basilar membrane to have no coupling in the longitudinal direction. Neglecting both fluid viscosity and partition damping, they obtained a numerical solution for the basilar membrane motion.

Ranke (1950) believed that waves in the cochlea were long in the basal region and short near the characteristic place. He developed a short-wave model in which he assumed the wave length to be short throughout and the fluid to be incompressible and inviscid. He compared his results to those of von Békésy.

The next significant step in the direct observation of the basilar membrane displacement was the introduction of the Mössbauer technique by Johnstone and Boyle (1967). This technique was refined by Rhode (1971) who was able to measure both amplitude and phase of basilar displacement in living squirrel monkeys. An example of Rhode's experimental results is shown in Fig. 4. Rhode's results inspired new mathematical models of cochlear mechanics.

Lien and Cox (1973) developed a quite elaborate three-dimensional cochlear model based on hydrodynamical equations. However, in order to find solutions to the basilar membrane displacement, they were forced to make simplifications which reduced the model to one dimension. They showed that longitudinal coupling in the basilar membrane was insignificant for the parameters chosen.

Schroeder (1973) presented a simplified long-wave one-dimensional model with an electrical transmission line analogy. By assuming that the place of the basilar membrane motion scaled with frequency, he was

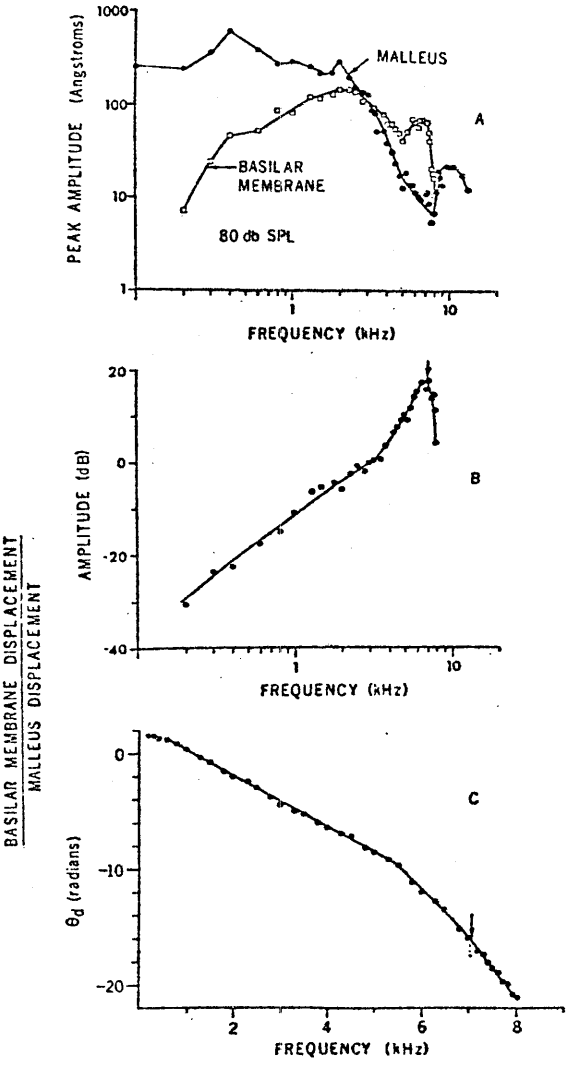

Figure 4. Rhode's experimental results using the Mössbauer technique on living squirrel monkeys. (a) Amplitude of vibration of the malleus and the basilar membrane versus frequency for a sound level pressure of 80 db SPL. (b) and (c) Amplitude and phase of the basilar membrane displacement to malleus displacement ratio. From Rhode (1971).

able to obtain analytical expressions for amplitude and phase slopes.

Siebert (1974) developed a two-dimensional model assuming an incompressible, inviscid fluid. His model took the form of an integral equation which he related to the long-wave model of Zwislocki (1965) and the short-wave model of Ranke (1950). Siebert made a short-wave approximation before finding solutions to his model.

Steele (1974) was concerned with structural features within the cochlea. He modeled the basilar membrane as a tapered plate immersed in a fluid and analyzed the fluid-elastic interaction for various approximations.

Zweig, Lipes, and Pierce (1976) improved on Schroeder's model by using a WKB approximation on the transmission line equations. They compared plots of numerical solutions with data due to Rhode.

Inselberg and Chadwick (1976) developed a two-dimensional model with viscous, incompressible fluid. They represented the basilar membrane as a beam with only longitudinal stiffness and obtained numerical solutions.

Allen (1977) was able to solve, numerically, the integral equation which was a key part of Lien and Cox's model. Allen presented numerical results for the two-dimensional cochlear model filled with an inviscid, incompressible fluid. His results appear to be the most accurate mathematical representation of cochlear mechanics yet published. Fig. 5 compares results of Zweig's model and Allen's model with experimental data of Rhode.

Non-linearities in the basilar membrane motion are also of interest. The basilar membrane displacement was observed by von Békésy to be a

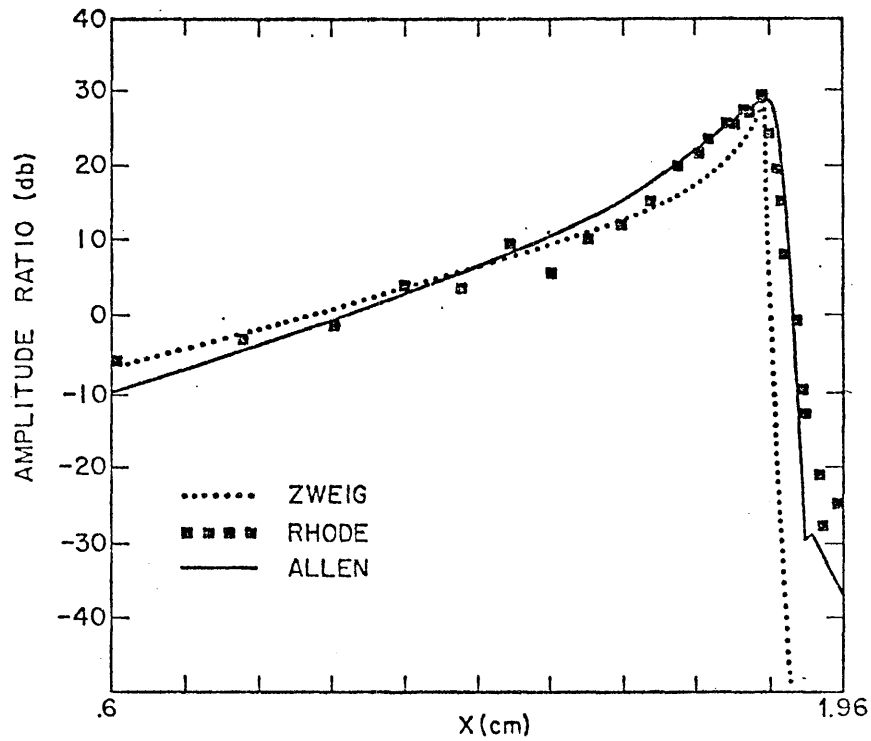

Figure 5. Amplitude of basilar membrane displacement ratios as computed by Allen, as computed by Zweig et al., and as measured by Rhode. From Allen (1977).

linear function of the loudness of the stimulus. Rhode and Robles (1974) observed non-linearities in the displacement for the living squirrel monkey, which were not present when the monkey died. Other evidence for non-linearities in hearing comes from psychoacoustic experiment. A non-linear loss mechanism was proposed by Kim, Molnar, and Pfeiffer (1973) and found to account for the known non-linearities. Hall (1974) used a non-linear damping parameter to match the non-linearities observed by Rhode (1971).

There are other sources of experimental data which depend indirectly on cochlear mechanics and should eventually be taken into consideration. Most important is the psychoacoustic evidence of hearing perception. The ear is remarkable in its ability to distinguish frequency differences and operate over a very wide dynamic range. Other experimenters have provided voluminous measurements of the activity of the auditory nerve in response to various acoustic stimulations. There is electrical activity in the cochlea other than that of the nerve cells; measurement of cochlear potentials provides another source of experimental data. For further discussion of these aspects of hearing research, the reader is referred to Zwicker and Terhardt (1974) or Schroeder (1975).

3. THE TWO-DIMENSIONAL MATHEMATICAL MODEL

A two-dimensional mathematical model of the cochlea will be developed from a consideration of the principal physical features of the human cochlea. The objective of this model is to provide a means of solving for the basilar membrane displacement when the stapes is vibrating with a sinusoidal motion. The entire cochlear partition is assumed to move as the basilar membrane. The mathematical development follows Peterson and Bogert (1950), Lien and Cox (1973), Siebert (1974), and Allen (1977).

As a first step in simplifying the cochlear structure, we consider the cochlea to be extended in a straight line, as shown in Fig. 6, instead of being curled into a spiral. The cochlea is coiled in most mammals, providing a more rigid structure, but the coiling arrangement apparently has no effect on the propagation of the acoustic wave in the cochlear fluid (Lien and Cox, 1973). Coordinate axes are also introduced in Fig. 6. The x-axis is perpendicular to the basilar membrane, the y-axis runs longitudinally along the cochlea, and the z-axis runs transversely across the cochlea.

The next simplification is to consider only the x and y-dimensions of the cochlea and assume there is no variation of any quantity in the z-direction. A two-dimensional representation of the cochlea is shown in Fig. 7.

The fluid which fills the cochlea is assumed to be incompressible and inviscid. The fluid will pass freely through the helicotrema as it does in the actual cochlea. The basilar membrane is an elastic partition

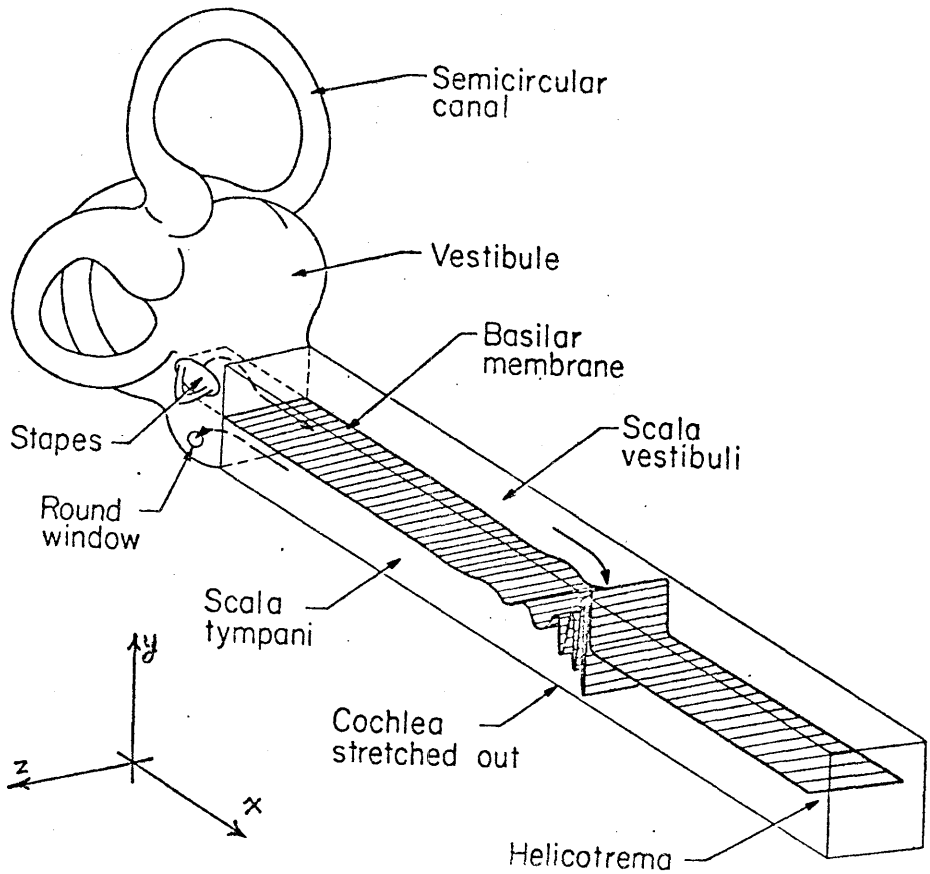

Figure 6. Simplified three-dimensional physical model of the cochlea. The cochlea is uncoiled and approximated by two fluid-filled, rigid-walled compartments separated by the basilar membrane. From Zweig et al. (1976).

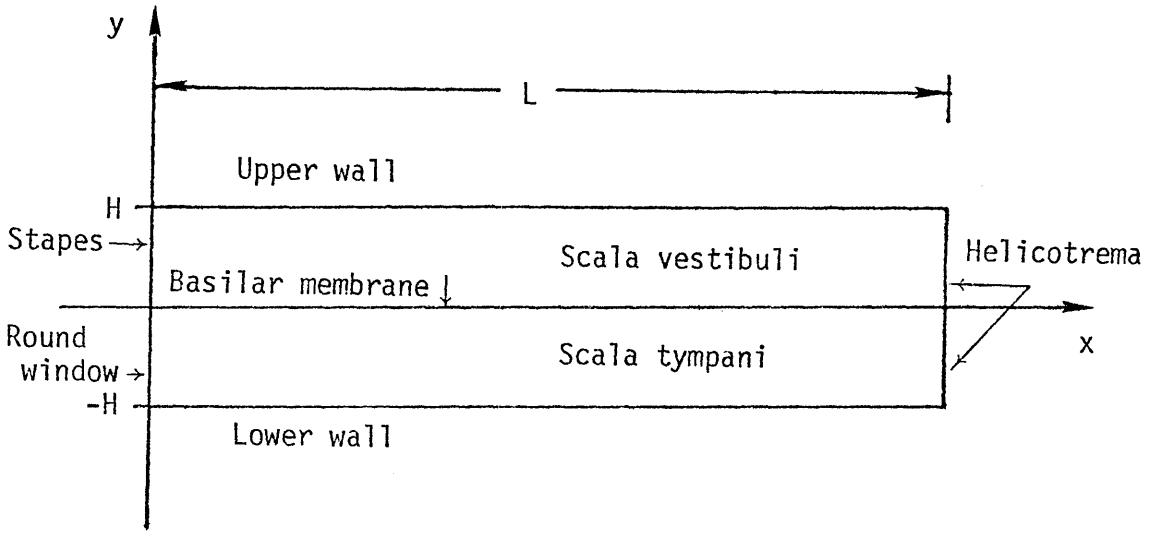

Figure 7. Two-dimensional representation of the cochlea. Two fluid-filled canals, the scala tympani and the scala vestibuli, are bounded by an upper and lower rigid wall and separated by the basilar membrane. The height of each canal is H and its length is L. The stapes and round window vibrate out of phase with each other and the helicotrema provides a connecting passage between the scalae.

between the two scalae which will be deformed by a pressure difference across it. The round window is assumed to be displaced by an amount equal to the displacement of the stapes in response to a sound signal.

The upper and lower walls in Fig. 7 represent the bony walls of the cochlea and will be assumed to be perfectly rigid. The height, H, of both scalae will be the distance from the basilar membrane to the rigid wall. The length, L, will be the distance from the stapes to the helicotrema.

These basic assumptions are the classical ones (Siebert, 1974 and Allen, 1977) and a discussion of their validity will be deferred to section 8.1. With these assumptions it will be possible to express our model equations entirely in terms of the pressure difference across the basilar membrane. We will proceed to discuss the fluid dynamics in such a two-dimensional region.

3.1 Cochlear hydrodynamics

The approach will be to specify the pressure $P(x,y,t)$ and vector velocity $\underline{V}(x,y,t)$ at each point in the fluid. The fluid is assumed to be incompressible, inviscid, and homogeneous with volume density, ρ. Since every differential volume of fluid is incompressible, we have, by continuity

$$\nabla \cdot \underline{V}(x,y) = 0. \tag{3.1}$$

From conservation of momentum applied to the differential volume

$$\rho \frac{d\underline{V}}{dt}(x,y) = - \nabla P(x,y). \tag{3.2}$$

Eq.(3.2) is our equation of motion; the time derivative is the substantial or material derivative (Huebner, 1975). If the velocity has an x-component u(x,y,t) and a y-component v(x,y,t) then

$$\frac{d\underline{V}}{dt} = \frac{\partial \underline{V}}{\partial t} + u\frac{\partial \underline{V}}{\partial x} + v\frac{\partial \underline{V}}{\partial y} . \tag{3.3}$$

Since the velocity of the fluid in the cochlea is very small under normal hearing conditions, we will linearize the equation of motion by assuming that

$$\frac{d\underline{V}}{dt} = \frac{\partial \underline{V}}{\partial t} . \tag{3.4}$$

In this case, we can take the divergence of both sides of eq.(3.2) to obtain

$$\nabla^2 P(x,y) = 0, \tag{3.5}$$

that is, the pressure in the fluid satisfies Laplace's equation. Note that eq.(3.5) depends on our assumptions of incompressibility and linearity, but not on our inviscid assumption.

Any dependence on time will be simplified by considering only sinusoidal displacements of the stapes. Only single frequency tones will be considered and the frequency will be varied as a parameter, ω. To implement this assumption of harmonic time dependence, we let P(x,y) and $\underline{V}(x,y)$ be complex functions such that

$$P(x,y,t) = \mathrm{Re}\left[P(x,y)e^{i\omega t}\right]$$

$$\underline{V}(x,y,t) = \mathrm{Re}\left[\underline{V}(x,y)e^{i\omega t}\right] \tag{3.6}$$

In the remainder of the thesis P and $\underline{V}$ will refer to the complex functions of pressure and velocity. Our basic fluid eqs.(3.1) and (3.2) can now be written as

continuity:
$$\frac{\partial u}{\partial x}(x,y) + \frac{\partial v}{\partial y}(x,y) = 0 \tag{3.7}$$

motion:
$$\frac{\partial P}{\partial x}(x,y) = -i\omega\rho u(x,y) \tag{3.8}$$

$$\frac{\partial P}{\partial y}(x,y) = -i\omega\rho v(x,y) \tag{3.9}$$

3.2 Mathematical formulation

We will use the hydrodynamic equations of section 3.1 to describe the pressure in each scala and then use the pressure difference across the basilar membrane to formulate our model equations. Let $P_v(x,y)$ describe the pressure of the fluid in the scala vestibuli and let $P_t(x,y)$ describe the pressure in the scala tympani. We assume that each scala has the same effect on the basilar membrane and consider the pressure distributions to be mirror images

$$P_v(x,y) = -P_t(x,-y). \tag{3.10}$$

This assumption is substantiated by von Békésy's observation that the round window vibrates exactly out of phase with stapedial footplate and with equal volume displacement.

From eq.(3.5) we have in the cochlear fluid

$$\nabla^2 P_v(x,y) = \nabla^2 P_t(x,-y) = 0. \tag{3.11}$$

Let u_s be the velocity of the stapes and u_r be the velocity of the round window. We assume the velocity of the fluid at these two boundaries is entirely in the x-direction. In order to normalize our solutions to unit displacement at the stapes for all frequencies, we set

$$u_s = -u_r = -i\omega. \tag{3.12}$$

From eq.(3.8) we have

$$\frac{\partial P_v}{\partial x}(0,y) = -\frac{\partial P_t}{\partial x}(0,-y) = -\omega^2\rho. \tag{3.13}$$

Let $v_b(x)$ be the velocity of the basilar membrane. We assume that the basilar membrane has only a y-component to its velocity. From eq.(3.9)

$$\frac{\partial P_v}{\partial y}(x,0) = -\frac{\partial P_t}{\partial y}(x,0) = -i\omega\rho v_b(x). \tag{3.14}$$

Along the rigid upper and lower walls, the y-component of the velocity must be zero. Hence, from eq.(3.9)

$$\frac{\partial P_v}{\partial y}(x,H) = \frac{\partial P_t}{\partial y}(x,-H) = 0. \tag{3.15}$$

The helicotrema is the connecting passage between the scala vestibuli and the scala tympani. We will require the pressures to be

equal across the helicotrema,

$$P_v(L,y) = P_t(L,-y). \tag{3.16}$$

We will proceed to define $P_d(x,y)$ as the "pressure difference" between the scala vestibuli and the scala tympani,

$$P_d(x,y) = P_t(x,-y) - P_v(x,y)\,, \tag{3.17}$$

for $0 < x < L$ and $0 < y < H$. This pressure difference will create a force acting on the basilar membrane in the positive x-direction. We will use $P_d(x,y)$ to define our model equations. Eqs.(3.11) and (3.13) to (3.16) can be expressed in terms of $P_d(x,y)$ as

$$\nabla^2 P_d(x,y) = 0 \tag{3.18}$$

$$\frac{\partial P_d}{\partial x}(0,y) = 2\omega^2\rho \tag{3.19}$$

$$\frac{\partial P_d}{\partial y}(x,0) = 2i\omega\rho v_b(x) \tag{3.20}$$

$$\frac{\partial P_d}{\partial y}(x,H) = 0 \tag{3.21}$$

$$P_d(L,y) = 0. \tag{3.22}$$

We could now solve for $P_d(x,y)$ if we could express v_b in terms of P_d. In order to accomplish this task we need to characterize the complex structure of the basilar membrane by an acoustic admittance $Y(x)$, which can be determined by experiment. More specifically, we need an

expression of the form

$$v_b(x) = Y(x)P_d(x,0). \tag{3.23}$$

In order to obtain this relation, we observe that the force which causes the basilar membrane to deflect at any point is given by the pressure difference between the two scalae at that point. Thus,

$$P_d(x,0) = M\frac{dv_b}{dt} + Rv_b + K\int^t v_b dt \tag{3.24}$$

where M(x), R(x), and K(x) are the mass, damping, and stiffness of the basilar membrane per unit area. The fundamental assumption underlying this equation is that an element of the basilar membrane dx have no direct mechanical coupling to neighboring elements (Peterson and Bogert, 1950). In accordance with our assumption of harmonic time dependence, eq.(3.24) becomes

$$P_d(x,0) = (i\omega M + R + K/i\omega)v_b(x). \tag{3.25}$$

From which we define our acoustic admittance function as

$$Y(x) = (i\omega M + R + K/i\omega)^{-1}. \tag{3.26}$$

3.3 Summary of model equations

In summary, our two-dimensional mathematical model is based on the following equations.

In the fluid, $0 < x < L$ and $0 < y < H$,

$$\nabla^2 P_d(x,y) = 0. \tag{3.27}$$

At the stapes, $x = 0$ and $0 < y < H$,

$$\frac{\partial P_d}{\partial x}(0,y) = 2\omega^2\rho. \tag{3.28}$$

Along the basilar membrane, $0 < x < L$ and $y = 0$,

$$\frac{\partial P_d}{\partial y}(x,0) = 2i\omega\rho Y(x)P_d(x,0). \tag{3.29}$$

Along the upper wall, $0 < x < L$ and $y = H$,

$$\frac{\partial P_d}{\partial y}(x,H) = 0. \tag{3.30}$$

At the helicotrema, $x = L$ and $0 < y < H$,

$$P_d(L,y) = 0. \tag{3.31}$$

When these equations have been solved for the pressure difference across the basilar membrane $P_d(x,0)$, we can find the displacement of the basilar membrane by

$$D(x) = v_b(x)/i\omega = Y(x)P_d(x,0)/i\omega. \tag{3.32}$$

Our model is normalized to unit displacement at the stapes, so D(x) represents the ratio of basilar membrane displacement to stapes displacement. Numerical solutions for D(x) will be presented in section 6.1.

4. THE INTEGRAL EQUATIONS FOR THE INFINITE COCHLEA

One way to approach a solution of the model equations presented in chapter 3 is to reduce the problem to one variable by incorporating the y-dimension into an integral equation. Two ways of developing integral equations will be presented in this chapter for the simplified case of an infinitely long cochlea. The boundary conditions at the stapes and at the helicotrema are ignored in the infinite cochlea, so that the relation between the integral equations can be shown more easily. These boundary conditions can be re-introduced by taking a second derivative with respect to x of the final equation. In this chapter we will define P(x) as the pressure difference across the basilar membrane

$$P(x) = P_d(x,0). \tag{4.1}$$

4.1 Green's function approach

An integral equation is desired of the form

$$P(x) = -2i\omega\rho \int_{-\infty}^{\infty} G(x|\xi) v_b(\xi) d\xi, \tag{4.2}$$

where $G(x|\xi)$ is a Green's function (Weinberger, 1965). Physically, $G(x|\xi)$ is the velocity potential at x due to a unit velocity source at ξ.

Consider that $v_b(x) = 0$ on the basilar membrane except that $v_b(\xi) = 1$. The y-dimension boundary conditions will be met by

constructing an appropriate array of image sources in the ± y-direction. The two boundary conditions, $v(x,H) = 0$ for all x and $v(x,0) = 0$ for all $x \neq \xi$, require images to extend infinitely in the ± y-direction, each separated by a distance 2H. This array of image sources is illustrated in Fig. 8.

The velocity potential on the basilar membrane due to a single velocity source at $y = 2nH$ and $x = \xi$, we will call $g_n(x,\xi)$. The Green's function for a single velocity source resting on a single rigid wall will be (Allen, 1977)

$$g_n(x|\xi) = -\frac{1}{2\pi} \ln\left[(x-\xi)^2 + (2nH)^2 \right] \qquad (4.3)$$

$$n = 0, \pm 1, \pm 2, \ldots$$

The total Green's function for the infinite cochlea will be the summation over all images:

$$G'(x|\xi) = -\frac{1}{2\pi} \sum_{n=-\infty}^{\infty} \ln\left[(x-\xi)^2 + (2nH)^2 \right]. \qquad (4.4)$$

A modification to the Green's function is still required. The summation does not converge, but can be separated into a convergent part and a divergent part which is constant, independent of x

$$G'(x|\xi) = -\frac{1}{\pi} \left\{ \ln|x-\xi| + \sum_{n=1}^{\infty} \ln\left[1 + \left(\frac{x-\xi}{2nH}\right)^2 \right] + 2\ln(2nH) \right\} \qquad (4.5)$$

The last term inside the brackets can be dropped, since it is independent of x. After replacing the sum of the logarithm by a logarithm of a

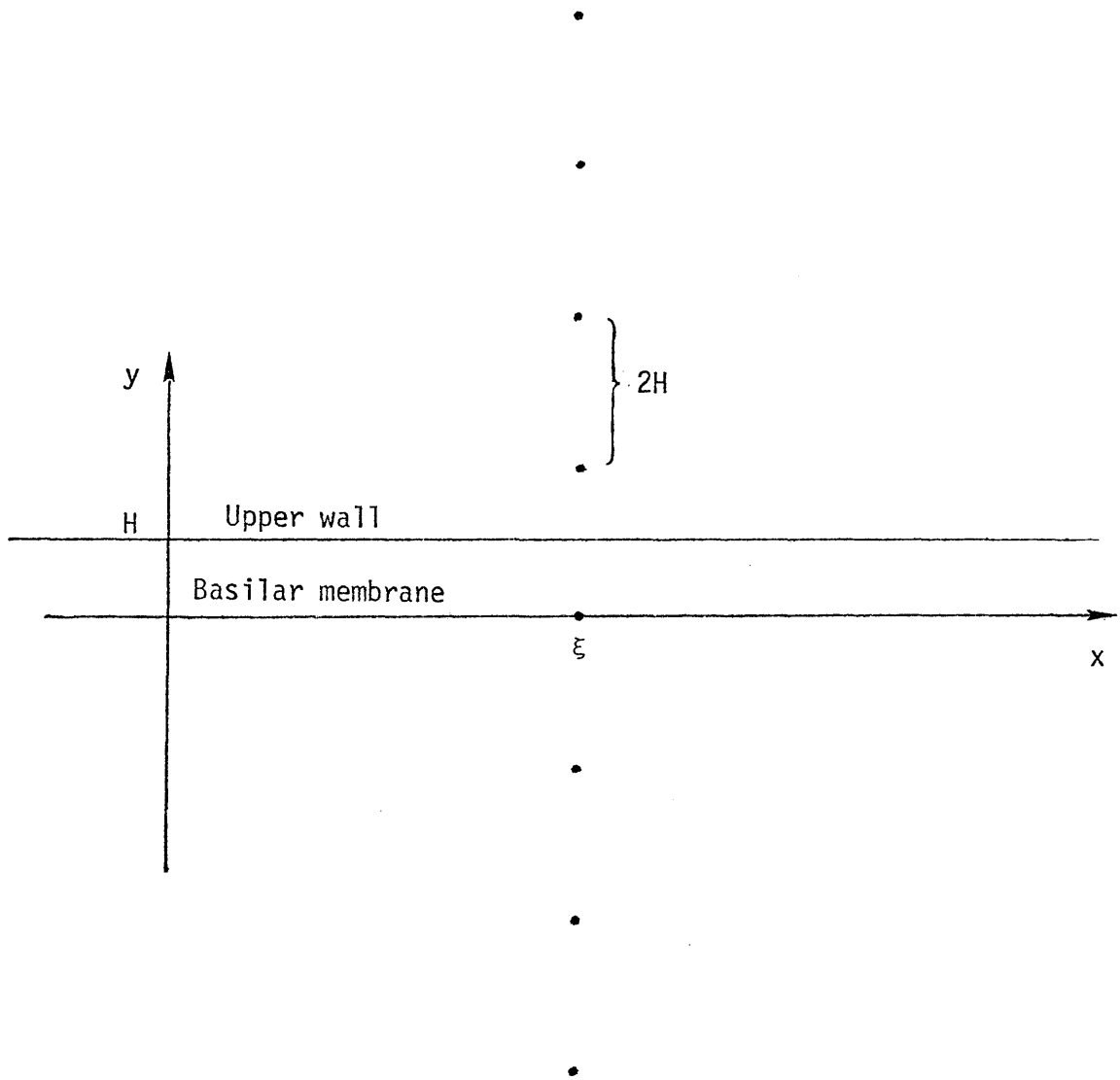

Figure 8. The velocity source resting on the basilar membrane at the point $x = \xi$, with some of the images used to meet the boundary conditions of a rigid upper wall and rigid basilar membrane. The images extend infinitely in the $\pm$ y-direction. The upper wall and basilar membrane extend infinitely in the $\pm$ x-direction.

product, our modified Green's function becomes

$$G(x|\xi) = -\frac{1}{\pi} \ln \left\{ |x-\xi| \prod_{n=1}^{\infty} 1 + \left(\frac{\pi(x-\xi)}{2H}\right)^2 \left(\frac{1}{n\pi}\right)^2 \right\}$$

$$= -\frac{1}{\pi} \ln \left\{ \sinh\left(\frac{\pi}{2H} |x-\xi|\right) \right\}, \qquad (4.6)$$

where the infinite product is replaced by the hyperbolic sine function (Gradshteyn and Ryzhik, 1965).

Integrating the velocity source over the entire basilar membrane gives the desired integral equation

$$P(x) = \frac{2i\omega\rho}{\pi} \int_{-\infty}^{\infty} \ln \left[\sinh\left(\frac{\pi}{2H}|x-\xi|\right) \right] Y(\xi)P(\xi)d\xi, \qquad (4.7)$$

where $v_b(\xi)$ has been replaced by the product of the basilar membrane admittance and the pressure difference according to eq.(3.23). The derivation of this equation follows the approach of Allen (1977) and Sondhi (1977). The stapes and the helicotrema boundary conditions are re-introduced by taking a second derivative of this integral equation with respect to x. When this is done, the resulting equation is a very good approximation to the two-dimensional model of chapter 3. The error is significant only for the pressure near the stapes and helicotrema boundaries.

The exact Green's function for the finite cochlea can be found in the same manner and can be expressed in terms of elliptic functions. Allen was able to solve numerically the integral equation, eq.(4.7),

modified for a finite length cochlea. An example of his numerical solution appears in Fig. 5.

4.2 Fourier transform approach

Another way to incorporate the y-dimension into an integral equation was published by Siebert (1974). The approach is to consider the traveling wave in the cochlea in terms of its sinusoidal components. We will define the spatial Fourier transform of P(x) as

$$p(\mu) = \int_{-\infty}^{\infty} P(x) e^{-i\mu x} dx. \tag{4.8}$$

In order to satisfy Laplace's equation in the fluid and the upper wall boundary condition, we require that

$$P_d(x,y) = \frac{1}{2\pi} \int_{-\infty}^{\infty} \frac{\cosh \mu(y-H)}{\cosh \mu H} e^{i\mu x} p(\mu) d\mu. \tag{4.9}$$

By applying the boundary condition on the basilar membrane, we have

$$2i\omega\rho Y(x)P(x) = \frac{-1}{2\pi} \int_{-\infty}^{\infty} \mu \tanh \mu H \, e^{i\mu x} p(\mu) d\mu. \tag{4.10}$$

Or by taking the Fourier transform of both sides of eq.(4.10), we have

$$\int_{-\infty}^{\infty} P(x) e^{-i\mu x} dx = \frac{-2i\omega\rho}{\mu \tanh \mu H} \int_{-\infty}^{\infty} Y(x) P(x) e^{-i\mu x} dx. \tag{4.11}$$

Siebert (1974) derived eq.(4.10) (modified for a finite cochlea) and noted its relationship to the long-wave and short-wave cochlear models, as well as the truncated Fourier series of Lesser and Berkley

(1972). This integral equation is closely related to the one-dimensional model of chapter 7.

4.3 Comparison of the integral equations

The two integral equations describe the same model of the cochlea and, hence, must be equivalent if they are correct. With slightly modified notation:

Allen's equation:

$$P(x) = \frac{2i\omega\rho}{\pi} \left\{ \ln\left[\sinh\frac{\pi}{2H}|x|\right] \right\} * Y(x)P(x) \qquad (4.12)$$

Siebert's equation:

$$\mathcal{f}\left[P(x)\right] = \frac{2i\omega\rho}{\mu \tanh \mu H} \cdot \mathcal{f}\left[Y(x)P(x)\right] \qquad (4.13)$$

where * denotes convolution and $\mathcal{f}[\cdot]$ denotes a spatial Fourier transform. Introducing the second derivative of P(x) with respect to x into both equations gives

$$\frac{d^2P}{dx^2}(x) = \frac{2i\omega\rho}{\pi} \left\{ \frac{d^2}{dx^2} \ln \sinh\frac{\pi}{2H}|x| \right\} * Y(x)P(x) \qquad (4.14)$$

$$\mathcal{f}\left[\frac{d^2P}{dx^2}(x)\right] = \frac{2i\omega\rho\mu}{\tanh \mu H} \cdot \mathcal{f}\left[Y(x)P(x)\right] \qquad (4.15)$$

Eq.(4.15) is the Fourier transform of eq.(4.14) provided that

$$\mathcal{f}\left[\frac{1}{\pi}\frac{d^2}{dx^2} \ln \sinh\frac{\pi}{2H}|x|\right] = \frac{\mu}{\tanh \mu H} \qquad (4.16)$$

We will proceed to verify eq.(4.16). First, note that

$$\frac{1}{\pi}\frac{d^2}{dx^2}\ln\sinh\frac{\pi}{2H}|x| = \frac{d^2}{dx^2}\left\{\frac{1}{2H}|x| + \frac{1}{\pi}\ln\left[1-\exp\left(-\frac{\pi}{H}|x|\right)\right]\right\}$$

$$= \frac{1}{H}\delta(x) + \frac{1}{\pi}\frac{d^2}{dx^2}\ln\left[1-\exp\left(-\frac{\pi}{H}|x|\right)\right] \qquad (4.17)$$

where $\delta(x)$ is the Dirac delta function. Substituting eq.(4.17) into eq.(4.16) and using the properties of the Fourier transform

$$f\left[\frac{1}{\pi}\frac{d^2}{dx^2}\ln\sinh\frac{\pi}{2H}|x|\right] = \frac{1}{H} - \frac{1}{\pi}\mu^2 f\left[\ln\left[1-\exp\left(-\frac{\pi}{H}|x|\right)\right]\right]$$

$$= \frac{1}{H} - \frac{2}{\pi}\mu^2\int_0^\infty \ln\left[1-\exp\left(-\frac{\pi}{H}x\right)\right]\cos\mu x dx$$

$$= \frac{1}{H} - \frac{2}{\pi}\mu^2\left\{\frac{\pi}{2H\mu^2} - \frac{\pi}{2\mu\tanh\mu H}\right\}$$

$$= \frac{\mu}{\mu\tanh\mu H}. \qquad (4.18)$$

Hence, the equivalence of Allen's equation and Siebert's equation is demonstrated. Evaluation of the integral in eq.(4.18) may be found in Gradshteyn and Ryzhik (1965) eq.4.383.2.

5. FITTING THE EXPERIMENTAL DATA

Because our mathematical model was derived from physical principles, its parameters can be related directly to meaningful physical properties of the cochlea. The relationship is not completely satisfying, partly because of the many simplifying assumptions and partly due to the sparsity of physical measurements available. Our choice of parameters will be presented in this chapter and numerical solutions for the displacement of the basilar membrane in chapter 6.

5.1 Physical dimensions

Our model reduces the complex physical structure of the cochlea to two parameters, the length L and height H. According to von Békésy (1960), the average length of the cochlea is 35 mm and the average height of the canal is 1 mm. These are the parameters we will use for our numerical solution. The more significant of these two parameters is the height. The height represents the vertical diameter of the roughly circular canal. The solutions of our mathematical model are much more sensitive to the height of the canal than to its length.

The density of the cochlear fluid is approximately the same as water. Hence, we choose $\rho = 1$ gm/cm^3.

5.2 The admittance function

In section 3.2 we made the assumption that the velocity at a given point on the basilar membrane is proportional to the pressure difference at that point. With this assumption we are able to incorporate the

complexity of the entire cochlear partition into an admittance function, Y(x). The admittance has the following form

$$Y(x) = \left[i\omega M(x) + R(x) + K(x)/i\omega \right]^{-1} \tag{5.1}$$

where M(x), R(x), and K(x) are the mass, damping, and stiffness of the basilar membrane per unit area and ω is the radian frequency of vibration.

Our choice for the mass, damping, and stiffness is the following

$$M(x) = 0.15 \text{ gm/cm}^2$$

$$R(x) = 200 \text{ dyn-sec/cm}^3$$

$$K(x) = 10^9 e^{-2x} \text{ dyn/cm}^3 \tag{5.2}$$

Our justification for this choice comes from a consideration of some experimental measurements of von Békésy. Our first interest was to approximate the cochlear map shown in Fig. 9.

The cochlear map shows the location of maximum activity on the basilar membrane due to a given sinusoidal tone. von Békésy's measurement of the location of maximum displacement is represented by the open circles. Localization from hearing loss measurements is represented by a dashed line. The "resonance" of our admittance function was chosen so that

$$f_r(x) = \frac{1}{2} \left(\frac{K}{M}\right)^{\frac{1}{2}} = 1.3 \times 10^4 e^{-x} \text{ Hz.} \tag{5.3}$$

If this function were plotted on Fig. 9, it would be a straight line which would lie on top of the dashed line. Instead, we plot the location

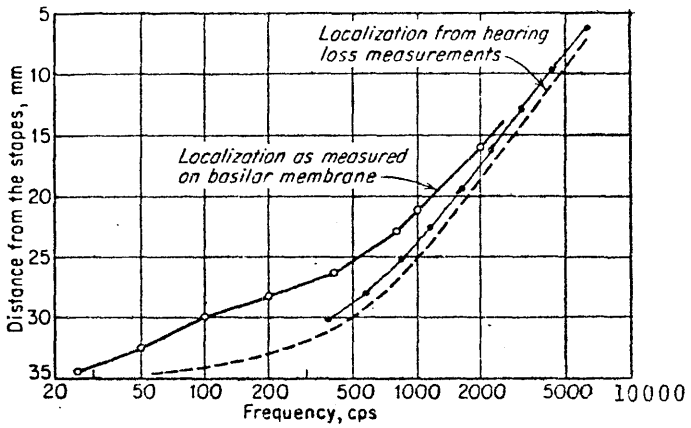

Figure 9. The cochlear map. Comparison of localization of tonal action on the basilar membrane. The open circles represent the direct observation of von Békésy, the dashed line was derived from measurement of hearing loss, and the solid circles are the results of our two-dimensional model. Adapted from von Békésy (1960).

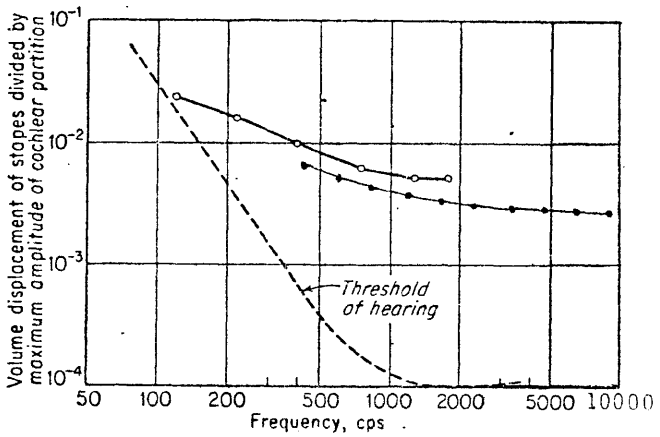

Figure 10. Ratio between the volume displacements of the stapes and the maximum amplitude of the cochlear partition as function of frequency. The open circles are the results of von Békésy's measurements. The closed circles are the results of our two-dimensional model assuming the cross-sectional area of scala vestibuli to be 1.5 sq. mm. Adapted from von Békésy (1960).

of the maximum displacement obtained by our numerical solution. This is represented by the solid circles in Fig. 9. The complete numerical solutions appear in chapter 6.

The damping, R(x), was chosen so that the amplitude of the maximum displacement would approximate von Békésy's data shown in Fig. 10. The open circles represent von Békésy's measurement and the solid circles represent our numerical solution, assuming the cross-sectional area of the canal to be 1.5 sq. mm.

The mass and damping were chosen to be constant for simplicity and from a consideration of the shape of the displacement amplitude and phase curves. The stiffness varies because the width of the basilar membrane changes. The basilar membrane is narrow near the stapes and wide near the helicotrema. Hence, the basilar membrane is stiffer near the stapes and more compliant near the helicotrema.

Table I gives a comparison of our admittance function with others that have been previously used. Allen's (1977) was "derived" by considering the basilar membrane as an inhomogeneous elastic plate with no stiffness in the longitudinal direction. Lien and Cox (1973) and Siebert (1974) used von Békésy's measurement of the static elasticity of the cochlear partition for their stiffness parameter. Peterson and Bogert (1950) used von Békésy's measurement of depression of basilar membrane due to a test hair for their stiffness. Damping and mass parameters tend to be unsubstantiated due to a lack of direct experiment measurement. In the case of Lien and Cox, the effective mass and damping were dependent on the viscosity of the fluid in a way which is not represented in Table I.

Table I. Comparison of Admittance Functions

	K(x)	R(x)	M(x)
Neely	$10^9 e^{-2x}$	200	0.15
Allen	$2 \times 10^9 e^{-3.4x}$	$600 e^{-1.7x}$	0.10
Lien and Cox	$8.6 \times 10^8 e^{-1.61x}$	600 x	0.2
Peterson and Bogert	$1.72 \times 10^9 e^{-2x}$	0	0.143
Siebert	$2 \times 10^8 e^{-1.5x}$	$5 e^{2.28x}$	0.01
units:	dyn/cm^3	$dyn\text{-}sec/cm^3$	gm/cm^2

For other aspects of basilar membrane modeling see Steele (1974), Allaire et al. (1974), and Novoselova (1975).

6. NUMERICAL SOLUTIONS OF THE TWO-DIMENSIONAL MODEL

In order to find solutions to the model equations of chapter 3, a two-dimensional finite difference scheme was used. In this chapter, plots of the numerical solutions are shown. Computation was performed on the Institute's time-sharing digital computer, a Digital Equipment Corporation PDP-10.

The pressure difference $P_d(x,y)$ was represented at a finite number of points in the fluid. Our two-dimensional array of points had 245 points in the x-direction and 8 points in the y-direction. Points had equal spacing in both directions, 7 points per millimeter. Finding the pressure difference at each point required solution of 1960 simultaneous equations. A description of the numerical procedure is given in Appendix A. On the PDP-10 computer, the solution for one set of parameters required about 70 seconds of CPU time.

6.1 Pressure, admittance, and displacement of the basilar membrane

Solutions to the two-dimensional model equations are presented in this section for the parameters described in chapter 5. The equations were solved for ten different frequencies separated by one-half octave intervals. The frequencies used were 0.40, 0.57, 0.80, 1.13, 1.60, 2.26, 3.20, 4.52, 6.39, and 9.04 kilohertz. The figures show ten plots superimposed.

The magnitude of the admittance $Y(x)$ is shown in Fig. 11a and the

phase in Fig. 11b. This represents the input function for our model equations and characterizes the assumed properties of the basilar membrane. The abscissa represents the x-dimension of our model. The ordinate shows the magnitude in decibels, $20 \log_{10}|Y(x)|$. All of the remaining figures follow this format to aid comparison.

The pressure difference across the basilar membrane is shown in Fig. 12. In Fig. 12a the functions plotted are $20 \log_{10}|P_d(x,0)|$. In Fig. 12b it was necessary to unwrap the phase so that it would not be restricted to $\pm \pi$. This was done in all phase plots subject to minimum phase slope.

The pressure distribution is multiplied by the admittance to give the y-velocity at the basilar membrane, From section 3.3 the y-displacement of the basilar membrane, relative to unit displacement at the stapes, is given by

$$D(x) = \frac{1}{i\omega} Y(x) P_d(x,0).$$

The magnitude and phase of the basilar membrane displacement are shown in Fig. 13. The displacement is shown as a function of distance from the stapes for ten frequencies as in Figs. 11 and 12.

In Fig. 14 the magnitude and phase of the displacement are shown as a function of frequency for six places on the basilar membrane. Fig. 14 required 100 separate solutions of D(x) for 100 different frequencies: only six points were kept from each solution. Approximately 7,000 seconds of processing time were required to prepare Fig. 14 as opposed to only 700 seconds for Fig. 13. For comparison experimental data due to Rhode are superimposed. (These are the same Rhode data shown in Fig. 5 and were taken from Zweig et al. (1976), Fig. 4).

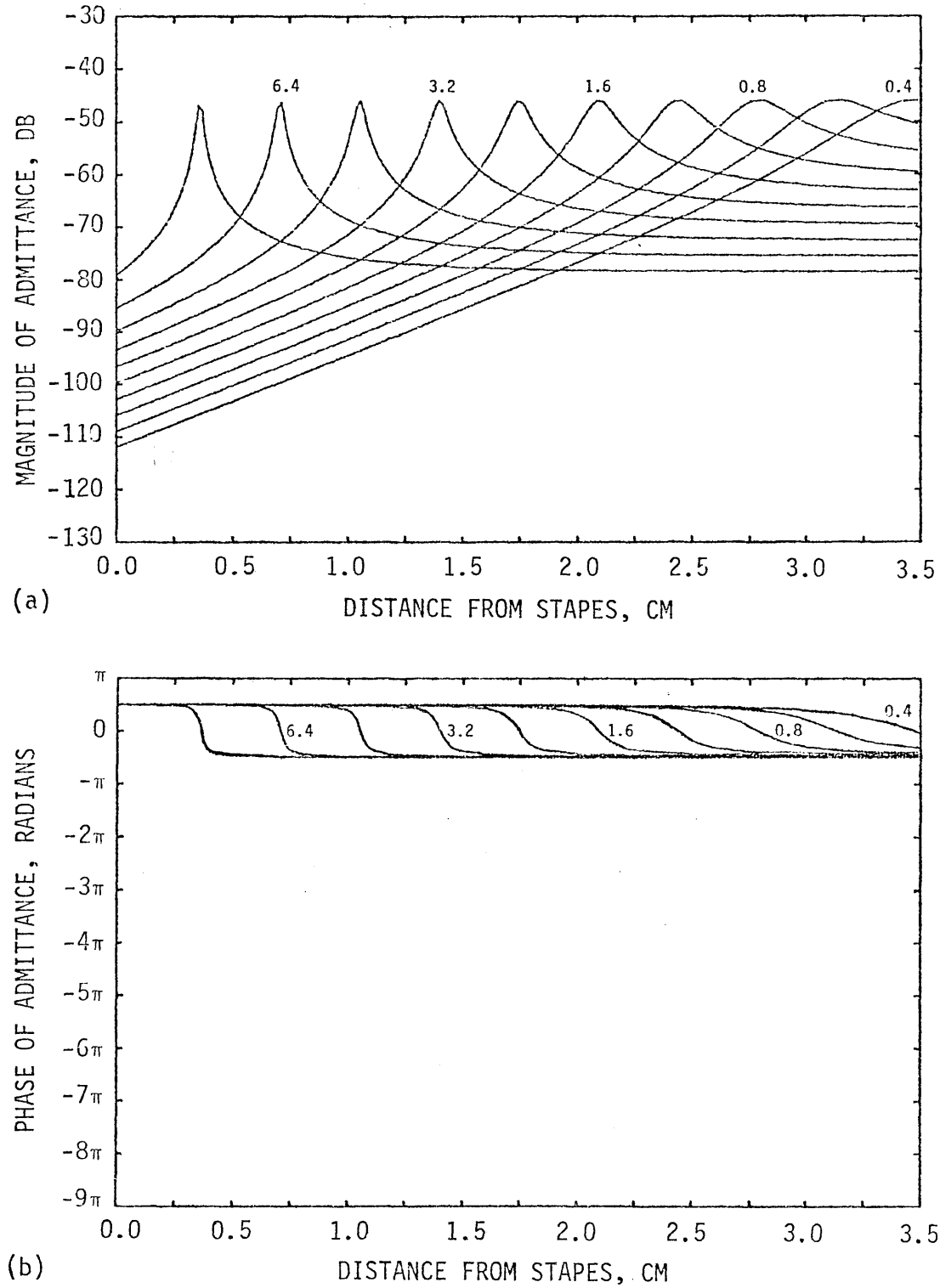

Figure 11. Basilar membrane admittance function as a function of distance from the stapes for ten frequencies: (a) magnitude and (b) phase. The magnitude curves are 20 $\log_{10}|Y(x)|$ and the phase curves are $\arg(Y(x))$. The numerals denote frequency in kilohertz.

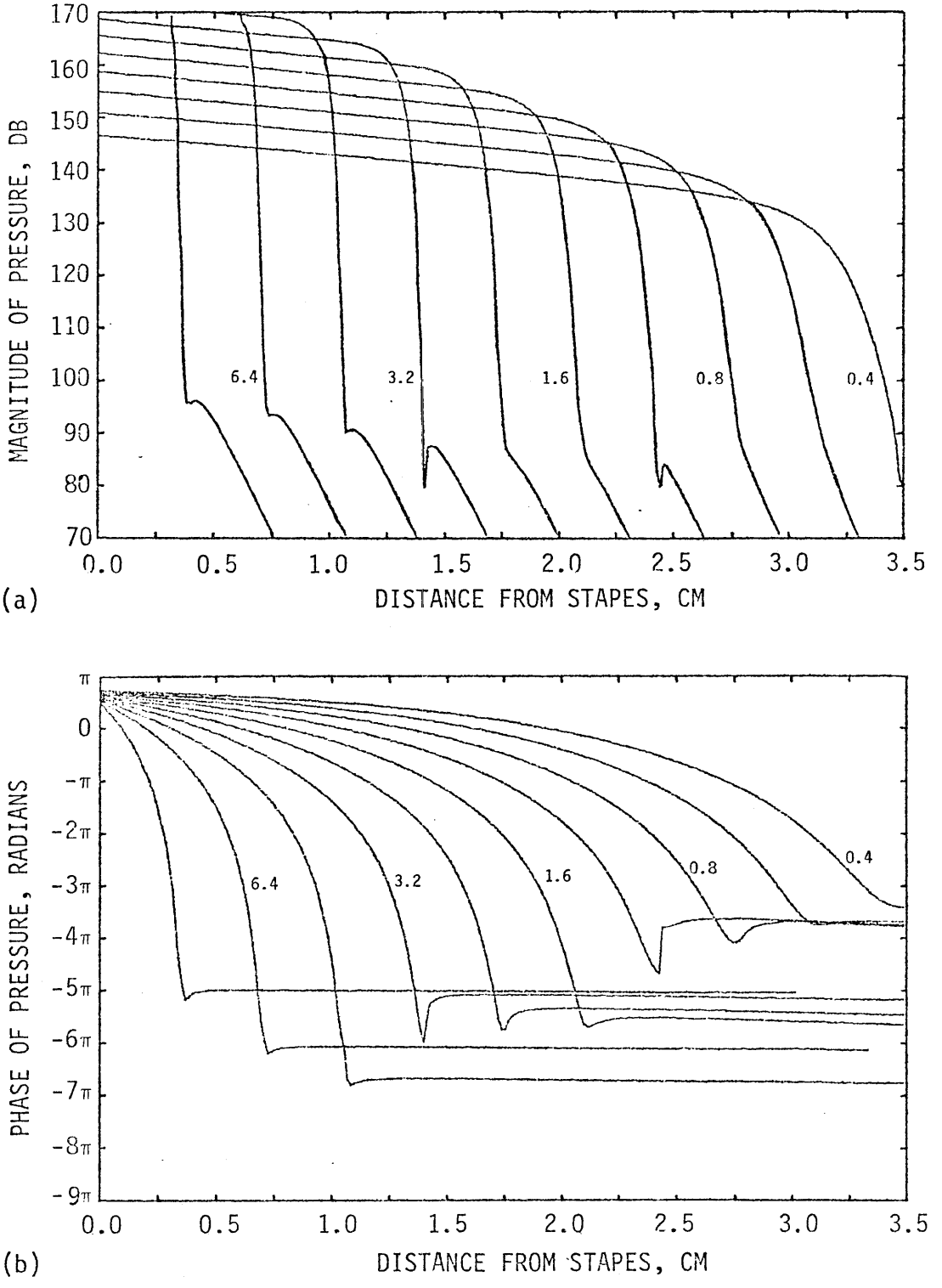

Figure 12. Pressure difference across the basilar membrane as a function of distance from the stapes for ten frequencies: (a) magnitude and (b) phase. The magnitude curves are $20 \log_{10}|P_d(x,0)|$ and the phase curves are $\arg(P_d(x,0))$. The numerals denote frequency in kilohertz.

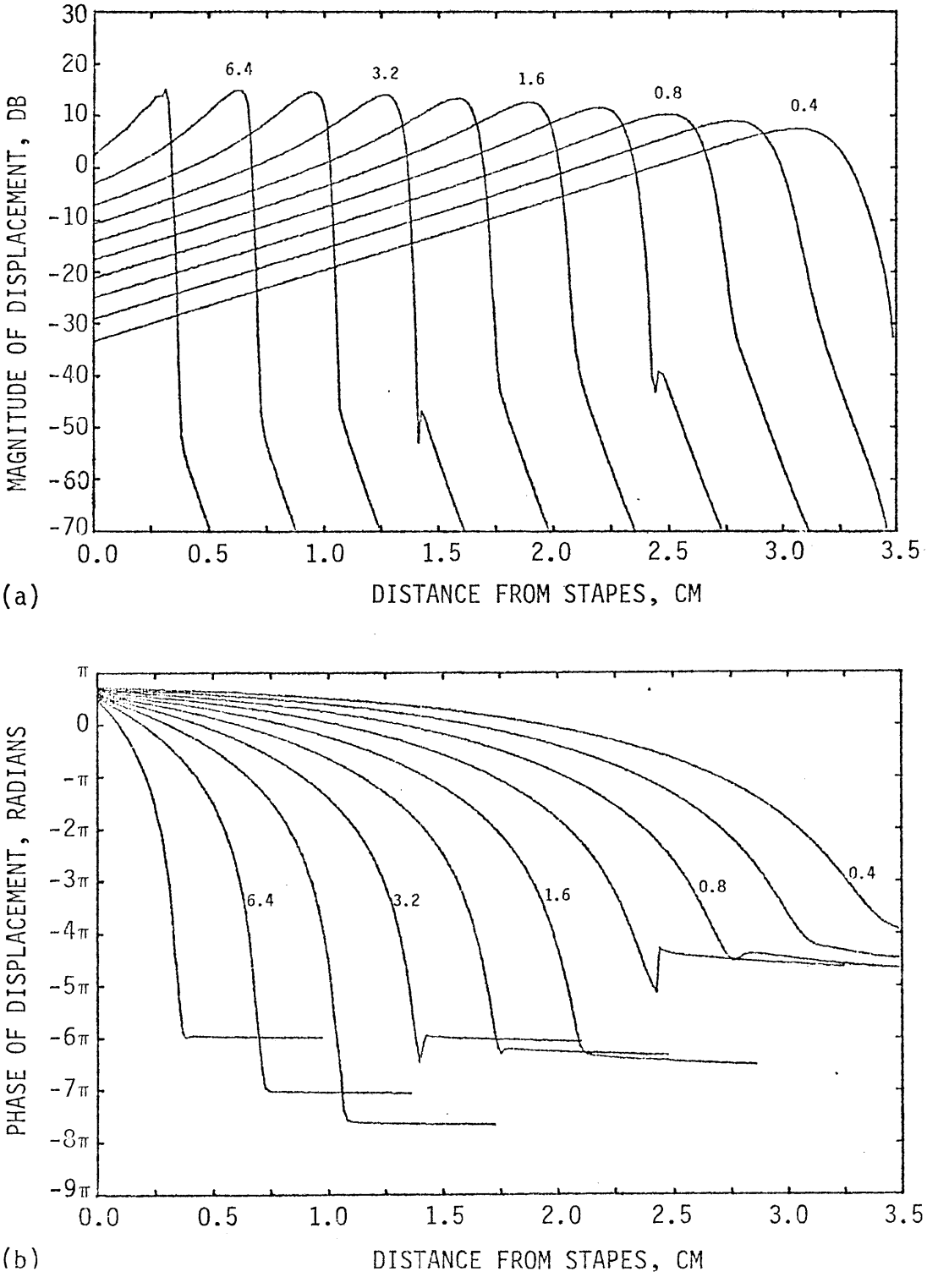

Figure 13. Basilar membrane displacement as a function of distance from the stapes for ten frequencies: (a) magnitude and (b) phase. The magnitude curves are 20 $\log_{10}|D(x)|$ and the phase curves are $\arg(D(x))$. The numerals denote frequency in kilohertz.

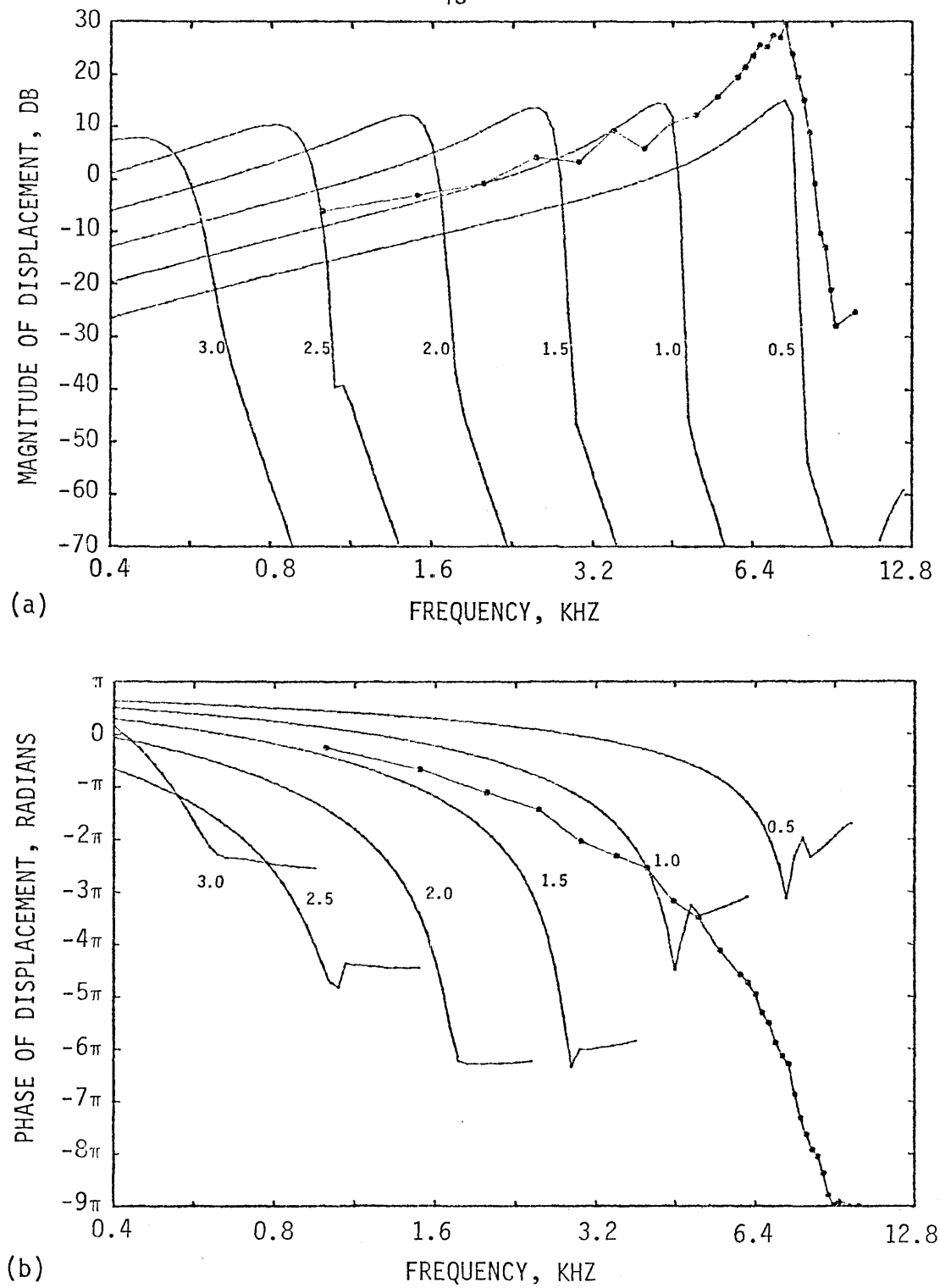

Figure 14. Basilar membrane displacement as a function of frequency for six positions along the cochlea: (a) magnitude and (b) phase. The numerals denote distance from the stapes in centimeters. The circles are Rhode's data from animal 69-473.

6.2 Variation of model parameters

Because of the degree of freedom in choosing the input parameters for this model, it seemed useful to show some of the results of varying the model parameters. The numerical solutions presented in this section are intended to provide a feeling for the range of solutions this model produces. Only plots of displacement versus distance from the stapes are shown in this section. They are comparable to Fig. 13 in section 6.1.

Much of the bony wall in the cochlea is closer to the basilar membrane than the one millimeter chosen as the height of the canal. Fig. 15 shows solutions when the height of the canal is set to one-half millimeter, H = 0.05 cm. The admittance function remains the same. For this solution we used 5 points in the y-direction and 280 points in the x-direction, that is, 8 points per millimeter.

Even if the stapes does not move hearing is possible through bone conduction (Wever, 1949). Fig. 16 shows solutions of our model with the stapes motionless and the upper wall vibrating sinusoidally with unit displacement. To accomplish this the boundary condition at the stapes and at the upper wall were interchanged. For clarity, only five frequencies are plotted in Fig. 16.

Fig. 17 shows solutions of our model for the parameters chosen by Allen (1977). These parameters were given in Table I in section 5.3. (It should be noted that there is a discrepancy of a factor of 2 between the numbers given in Table I which were found to fit Allen's curves and the numbers which Allen published.) Allen chose these parameters in such a way that the magnitude curves scale with frequency and are a close fit to the experimental data of Rhode (see Fig. 5).

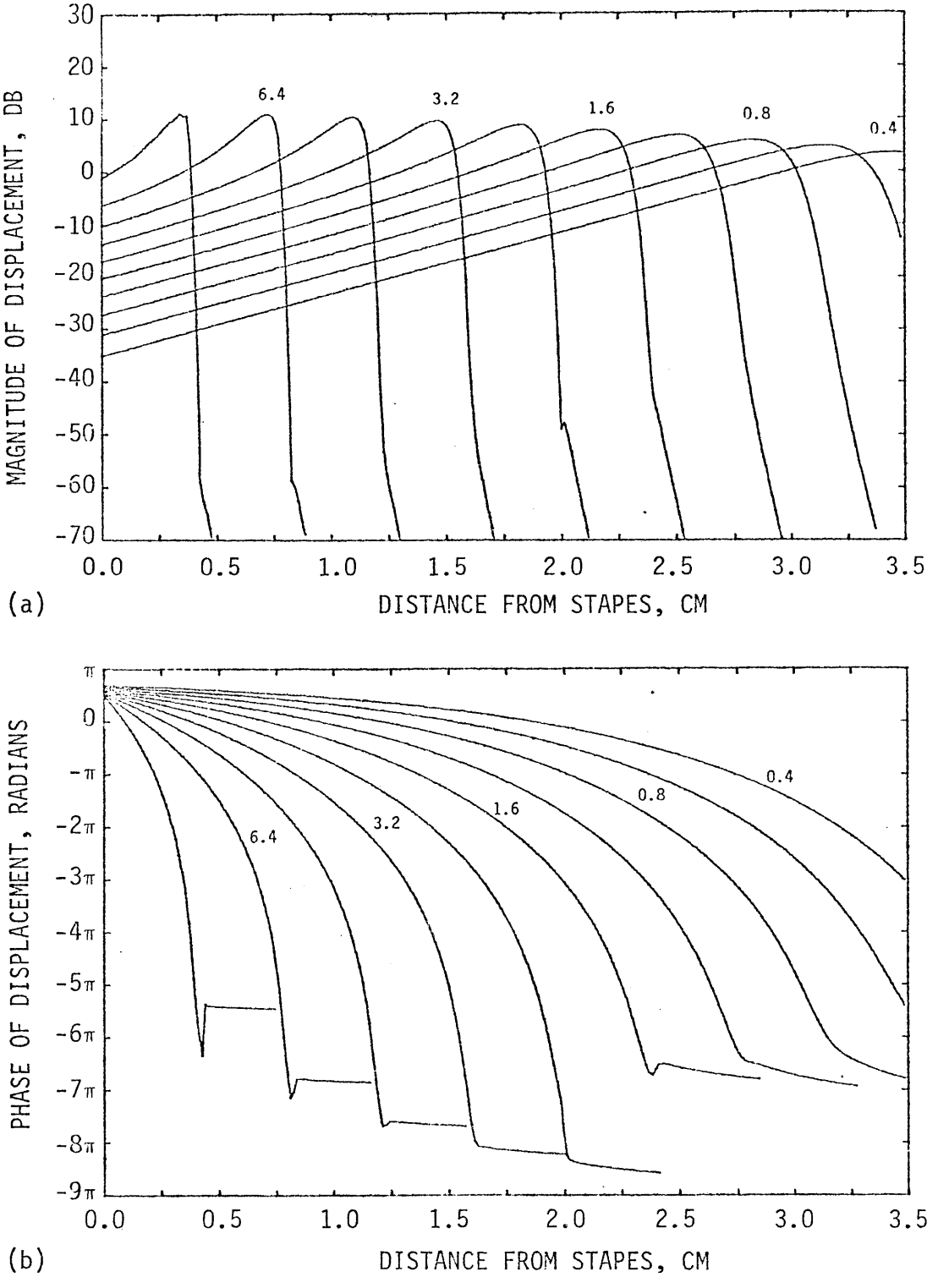

Figure 15. Basilar membrane displacement as a function of distance from the stapes: (a) magnitude and (b) phase. The height of the canal was reduced to 0.05 cm for this case. The numerals denote frequencies in kilohertz.

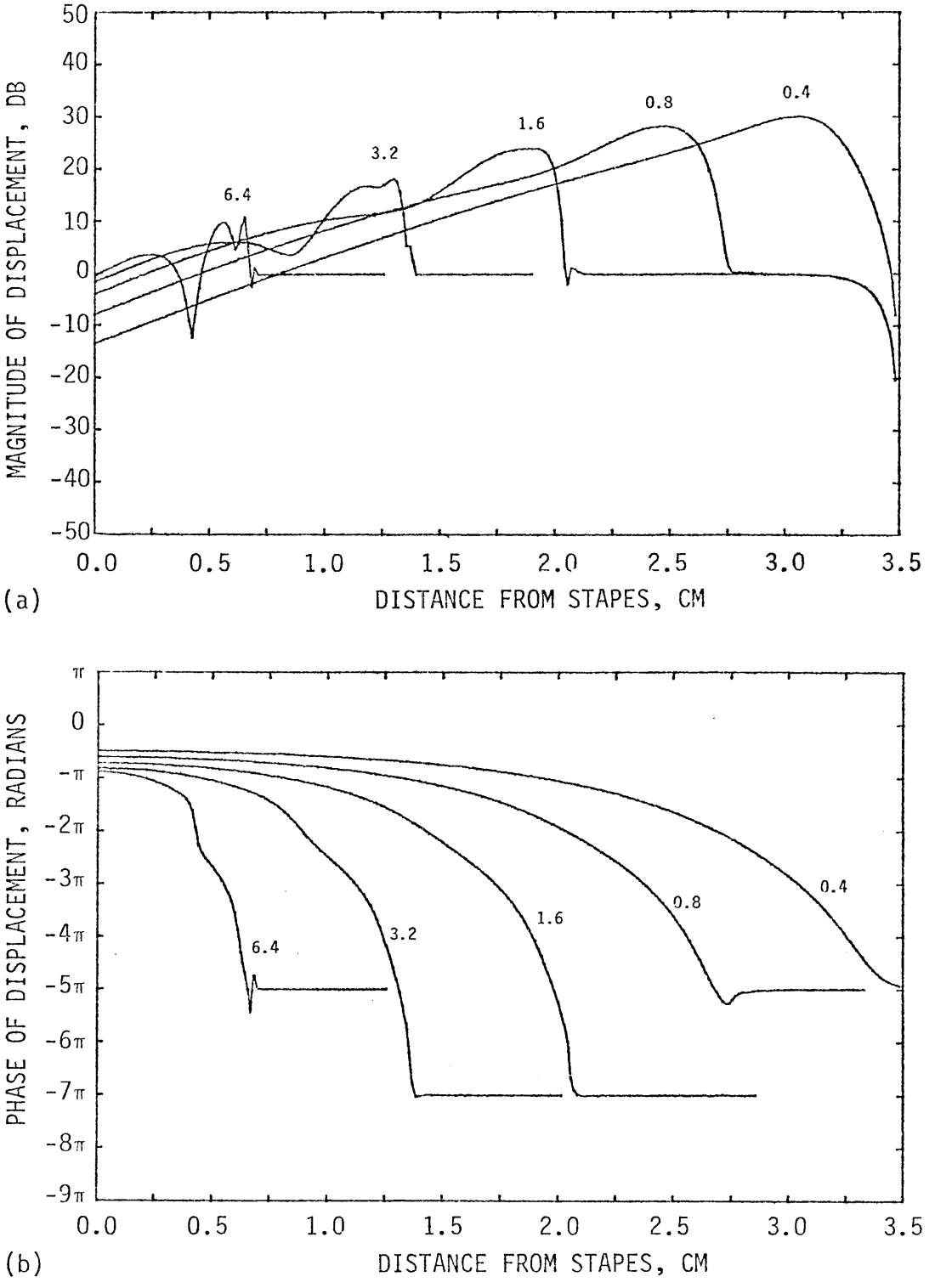

Figure 16. Basilar membrane displacement as a function of distance from the stapes: (a) magnitude and (b) phase. The stapes was rigid and the upper wall vibrating with unit displacement in this case. The numerals denote frequencies in kilohertz.

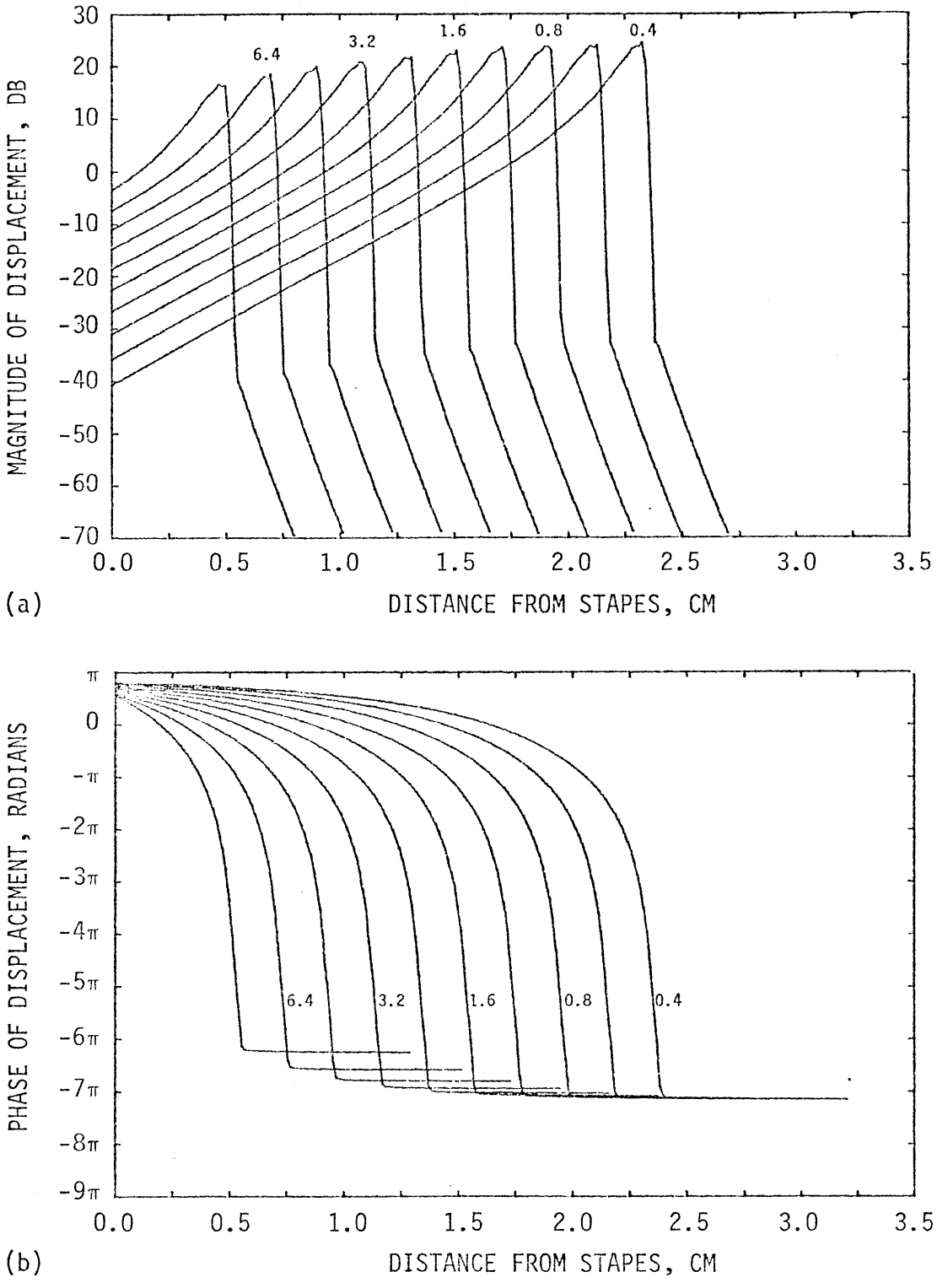

Figure 17. Basilar membrane displacement as a function of distance from the stapes: (a) magnitude and (b) phase. Allen's admittance function was used for this case. The numerals denote frequencies in kilohertz.

7. THE ONE-DIMENSIONAL MODEL

Our direct numerical solution of the two-dimensional model requires a large computer and provides limited insight into the mechanisms whereby the observed behavior is brought about. To overcome these limitations, a more approximate model of the cochlea is still useful.

Zweig, Lipes, and Pierce (1976) were able to derive an analytic representation for a one-dimensional model of the basilar membrane displacement by making a long-wave assumption and a WKB approximation. In this chapter a new one-dimensional model is presented. Our one-dimensional model is based on the two-dimensional model of chapter 3 and can be reduced to the model of Zweig, et al. The one-dimensional model is not as accurate as the two-dimensional model and does not lead to a completely analytic expression for the pressure distribution. Instead, it is a compromise which adds another bit of insight into the mechanics of the cochlea.

7.1 The "slowly varying" approximation

If the admittance of the basilar membrane were a constant

$$Y(x) = Y_0 \ , \tag{7.1}$$

an exact solution of the two-dimensional model equations is available. This situation is referred to as the untapered cochlea. For the infinite, untapered cochlea

$$P_d(x,y) = P_0 \cosh\left[\beta_0(y-H)\right] \ e^{-i\beta_0 x} \tag{7.2}$$

where

$$\beta_0 H \tanh \beta_0 H = -2\omega\rho Y_0 H. \tag{7.3}$$

We can verify that this expression satisfies Laplace's equation in the fluid and the desired boundary conditions at the basilar membrane and the upper wall. The pressure distribution and, hence, the displacement of the basilar membrane varies sinusoidally with x. If λ_0 is the wavelength on the basilar membrane, then $\beta_0 = 2\pi/\lambda_0$.

von Békésy (1960) observed the displacement of the basilar membrane to be approximately sinusoidal with slowly varying amplitude and phase. Thus, it seems reasonable that the pressure distribution in the tapered cochlea would be approximately be the same as the untapered cochlea within a limited range of x. We will assume that the y-variation of the pressure is that of the hyperbolic cosine:

$$P_d(x,y) = \cosh\left[\, \beta(x)(y-H)\right] P_d(x,H) \tag{7.4}$$

where

$$\beta(x)H \tanh \left[\beta(x)H\right] = -2i\omega\rho Y(x)H. \tag{7.5}$$

We expect that

$$P_d(x,H) \approx P_0 \exp\left[\, i\int^x \beta(x)dx \,\right]. \tag{7.6}$$

The function $P_d(x,H)$ will be approximately sinusoidal with varying amplitude and phase. The function $\beta(x)$ represents the complex "local wavenumber" of the disturbance on the basilar membrane. Laplace's equation in the fluid becomes

$$\frac{\partial^2 P_d}{\partial x^2}(x,y) + \beta^2(x) P_d(x,y) = 0. \qquad (7.7)$$

At this point we lose track of the y-dimension. Eq.(7.7) will have a solution for only one choice of y, unless $\beta(x)$ is a constant function. We assume that $P_d(x,y)$ as given by eqs.(7.5) and (7.7) will be approximately correct when $\beta(x)$ is slowly varying.

7.2 Model equations

We choose to solve eq.(7.7) for a single value of y, say $y = y_0$. The same boundary conditions as given in section 3.3 will be used at the stapes and the helicotrema. For convenience, we define $f(x) = P_d(x,y_0)$. The one-dimensional model is based on the following equations:

the transcendental equation

$$\beta(x) H \tanh \beta(x) H = -2i\omega\rho Y(x) H, \qquad (7.8)$$

the differential equation for $0 < x < L$

$$\frac{d^2 f}{dx^2}(x) + \beta^2(x) f(x) = 0, \qquad (7.9)$$

the stapes and helicotrema boundary conditions

$$\frac{df}{dx}(0) = 2\omega^2\rho \qquad (7.10)$$

$$f(L) = 0, \qquad (7.11)$$

and the pressure difference

$$P_d(x,y) = \frac{\cosh \beta(x)(y-H)}{\cosh \beta(x)(y_0-H)} f(x). \qquad (7.12)$$

The basilar membrane displacement, relative to unit displacement at the stapes, will be

$$D(x) = \frac{1}{i\omega} \frac{\cosh \beta(x)H}{\cosh \beta(x)(y_0-H)} Y(x)f(x). \qquad (7.13)$$

7.3 Numerical solutions for displacement of basilar membrane

The major difficulty in obtaining a solution to this one-dimensional model is the transcendental equation, eq.(7.8). When an approximate value for $\beta(x)H$ is known, an accurate solution of the transcendental equation can be obtained numerically by iteration. Appendix B discusses an iterative procedure and gives the Fortran code for the subroutine ATNH. A sample of computed values for βH in the vicinity of resonance is presented in Table II for a frequency of 1600 Hz. The values of βH could be verified by comparing the y-variation of $P_d(x,y)$ with the two-dimensional model.

The displacement of the basilar membrane for this one-dimensional model is shown in Fig. 18 for the same ten frequencies used in chapter 6. The parameters used are identical to those used in Fig. 13. There was one additional parameter which the two-dimensional model did not have, y_0. For the solutions shown in Fig. 18, $y_0 = 0$.

Table II. Sample Results of ATNH Subroutine

	$-2i\omega_p Y(x)H$		$\beta(x)H$	
x	real	imag.	real	imag.
0.00	0.021	-0.000	0.144	-0.000
0.01	0.021	-0.000	0.146	-0.000
0.03	0.022	-0.000	0.148	-0.000
...	...		...	
1.90	2.601	-0.725	2.613	-0.699
1.91	2.809	-0.858	2.813	-0.838
1.93	3.041	-1.025	2.040	-1.010
1.94	3.300	-1.235	3.295	-1.226
1.96	2.585	-1.503	3.580	-1.500
1.97	3.896	-1.851	3.893	-1.851
1.99	4.226	-2.305	4.225	-2.306
2.00	4.556	-2.902	4.556	-2.904
2.01	4.846	-3.691	4.846	-3.690
2.03	5.017	-4.717	5.017	-4.716
2.04	4.931	-6.003	4.931	-6.004
2.06	4.385	-7.485	4.385	-7.482
2.07	3.185	-8.917	3.163	-8.945
2.09	1.328	-9.875	1.830	-10.000
2.10	-0.812	-9.987	0.153	-1.542
2.11	-2.703	-9.265	0.147	-1.511
2.13	-4.001	-8.069	0.140	-1.482
2.14	-4.710	-6.783	0.134	-1.455
2.16	-4.991	-5.626	0.129	-1.430
2.17	-5.014	-4.666	0.124	-1.385
2.19	-4.898	-3.898	0.193	-1.365
2.20	-4.717	-3.290	0.149	-1.346
...	...		...	
3.46	-1.399	-0.199	0.044	-0.970
3.47	-1.396	-0.198	0.044	-0.969
3.49	-1.393	-0.197	0.044	-0.968

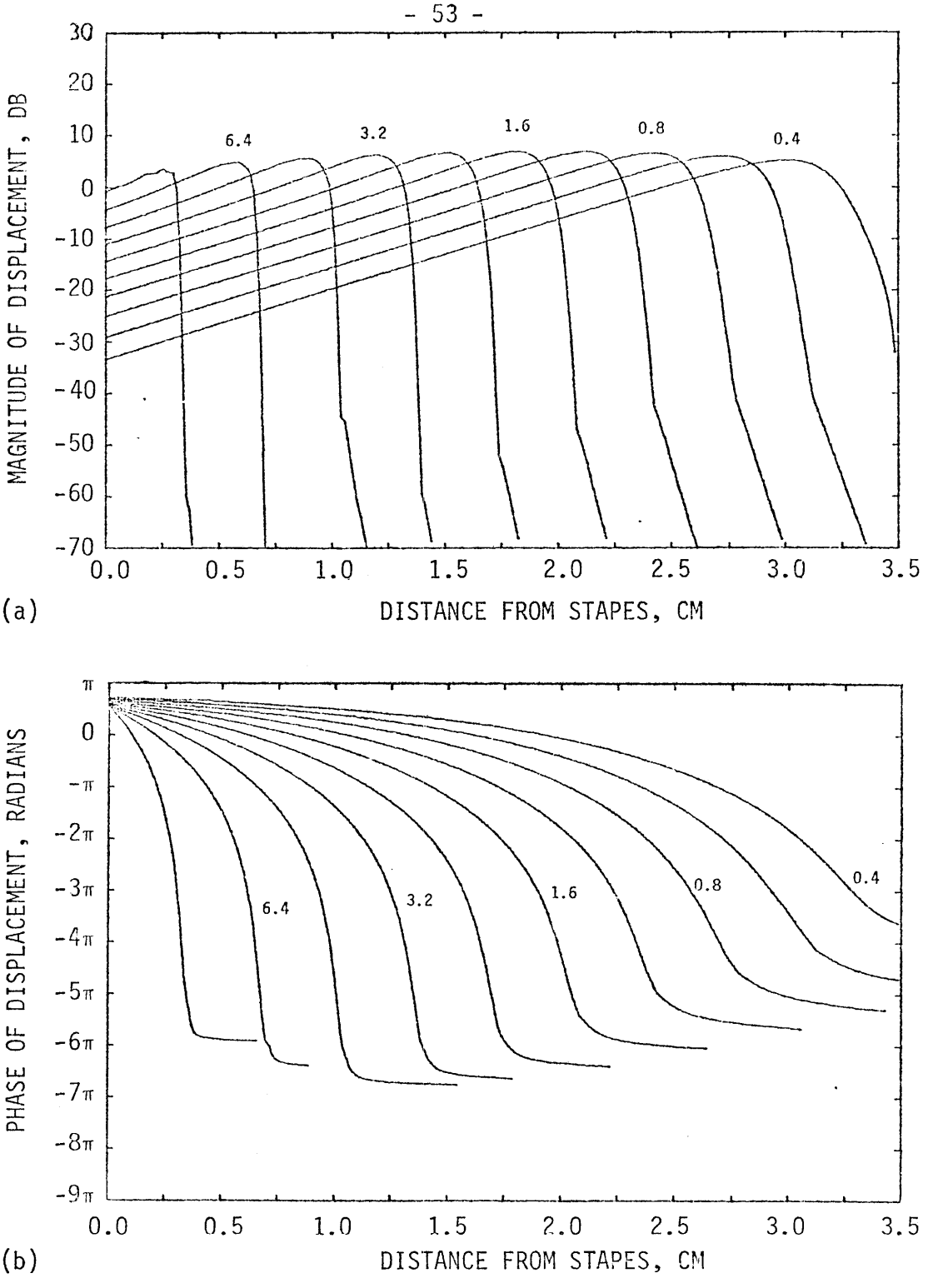

Figure 18. Basilar membrane displacement as a function of distance from the stapes: (a) magnitude and (b) phase. These curves are computed from our "slowly varying" model. The numerals denote frequencies in kilohertz.

7.4 The long-wave approximation

In section 7.1 we referred to $\beta(x)$ as the "local wavenumber,"

$$\beta(x) = 2\pi/\lambda(x) \tag{7.14}$$

where $\lambda(x)$ is the "local wavelength." When the wavelength is much greater than the height of the canal, the motion of the fluid is approximately independent of y. This makes the one-dimensional model much easier to solve. To be more precise, a long wave approximation requires that

$$\beta(x)H << 1. \tag{7.15}$$

When this is true $\tanh[\beta H] = \beta H$ and

$$\beta^2(x) = \left[\frac{-2i\omega\rho Y(x)}{H}\right] \tag{7.16}$$

For the long-wave approximation Laplace's equation requires only that

$$\frac{d^2P_d(x)}{dx^2} - 2\frac{i\omega\rho}{H}Y(x)P_d(x) = 0, \tag{7.17}$$

where the pressure difference $P_d(x)$ is now independent of y. Studies of this, or a very similar equation, have been published by many investigators. In particular the one-dimensional model of Zweig et al. (1976) takes the form of eq.(7.17). Note that eq.(7.17) is also a long-wave approximation of eq.(4.15).

8. DISCUSSION OF RESULTS

The foundation for the mathematical model presented in this thesis rests primarily on the work of previous authors, especially Allen (1977), Lien and Cox (1973), and Siebert (1974). The new developments are basically 1) a Fourier transform relationship between Allen's and Siebert's integral equations, 2) a faster and more direct numerical solution of the two-dimensional model, and 3) a one-dimensional model which gives some additional insight into the qualitative features of the basilar membrane motion.

8.1 Validity of basic assumptions

The tubular, coiled structure of the cochlea is represented by a rectangular region filled with an inviscid, incompressible fluid. The whole cochlear partition (including the basilar membrane, Reissner's membrane, and everything in between) is modeled as a succession of elastic points which are assumed to be not directly coupled to adjacent points. All motion is assumed to be linear and have harmonic time dependence. This is, admittedly, a drastic simplification of the physical cochlea. Our justification for these basic assumptions lies primarily in the extent to which they have become established in previous studies. We will discuss some of these assumptions in more detail.

The assumption that the fluid is incompressible is a good one. For an incompressible fluid the sound velocity is infinite. It would not

have been difficult to include a finite sound velocity in our model formulation, but its effect was found to be insignificant compared to other terms. Peterson and Bogert (1950) and Lien and Cox (1973) considered compressibility and found that the assumptions of incompressibility did not affect their results.

The assumption of an inviscid fluid is not so well substantiated. von Békésy measured the viscosity of the cochlear fluid and found it to be about twice that of water. Lien and Cox showed that with certain approximations the fluid viscosity was only significant in the vicinity of the boundaries. Hence, the effect of the fluid viscosity could be incorporated into the basilar membrane admittance function and would appear nowhere else in the model equations. A viscosity term was not included in our admittance function because its effect could be incorporated, for the most part, into the damping and mass parameters.

We follow Allen in assuming the pressure to be zero at the helicotrema. For frequencies above 400 Hz this boundary condition is of little consequence, because the pressure has dropped nearly to zero anyway due to losses in the basilar membrane. Below 400 Hz this boundary condition creates standing waves in the solution due to reflection of the wave at the helicotrema. This did not seem proper, so we simply avoided using frequencies below 400 Hz. In effect, we avoided the helicotrema boundary.

Actually, the stapes is not in line with the longitudinal direction of the cochlea. Instead it connects to the side of the vestibule as shown in Fig. 6. This boundary condition in our model translates to assuming that the fluid across the entrance of the cochlea moves in phase

and with unit displacement. The exact distribution of fluid motion across the entrance of the cochlea is relatively unimportant; other choices produced similar shaped curves for displacement of the basilar membrane.

The upper wall of the cochlea is certainly much more rigid than the fluid or the basilar membrane. Rhode (1971) found no motion of the temporal bone at any frequency as he measured the basilar membrane motion. The bony limbus, on the other hand, was found to vibrate about 16 db below the basilar membrane vibration. The major weakness of the rigid upper wall assumption is that it is all that remains in our two-dimensional model of the bony pod that encloses the physical cochlea.

Our representation of the basilar membrane has no longitudinal coupling within itself. It is analogous to a number of transverse beams which are not interconnected; the model has no stiffness in the longitudinal direction. Lien and Cox (1973) found this to be a reasonable assumption provided that the local wavelength is greater than twice the width of the basilar membrane. This condition is satisfied for the solutions of our model using the measurements of Wever (1949) for the width of the basilar membrane. More will be said about wavelength in section 8.2.

8.2 Comparison with experiment

Many hours were spent trying to find input parameters for our model which would produce solutions that fit the experimental data of von Békésy (1960) and Rhode (1971). A close fit to both magnitude and phase of Rhode's data was impossible, although either could be fitted separately

for suitable parameters. Finally, the admittance function was chosen so that the solutions would fit the cochlear map and compromise on fitting the basilar membrane displacement.

The results of our model for the lower frequencies as shown in Fig. 13 agree well with the results of von Békésy shown in Fig. 3b. The phase drops about 2π radians at the characteristic place for von Békésy's data at 300 Hz and for our results at 400 Hz. The basilar membrane motion becomes more localized with increasing frequency in both our model and von Békésy's data as shown in Fig. 3a.

A much closer comparison is possible with Rhode's data in Fig. 14. Rhode's curves are not exactly comparable for two reasons. Rhode's measurements are of living squirrel monkeys while our parameters were based on data obtained from human cadavers. The model displacement is measured relative to fluid motion at the stapes and Rhode's displacement is relative to vibration of the malleus. Evidently, the transformation from malleus displacement to stapes displacement is approximately independent of frequency up to a few kilohertz. Rhode found the incus to malleus displacement ratio to be about -6 db from 0 to 10 kilohertz; while the phase difference went from 0° to about 45°.

The magnitude curves for our model agree reasonably well with that of Rhode in Fig. 14a. The low frequency slopes are similar, there is an increase in slope near the characteristic frequency, and the decreasing slope beyond the characteristic frequency is quite steep. Also, there is the plateau, or at least a change in slope, about 60 db down from the peak on the high frequency side.

The phase curves in Fig. 14b do not agree so well. The phase of

our model results does not drop far enough and changes too abruptly at the higher frequencies. Allen (1977) had a similar problem in fitting his solutions to Rhode's data. Notice in Fig. 15b that reducing the height of the cochlear canal causes the phase to drop further and more gradually, more like Rhode's phase curves. Perhaps a three-dimensional model could fit both Rhode's magnitude and phase. The height of the canal cannot really be chosen properly for a two-dimensional model.

The local wavelength of the basilar motion at the characteristic place can also be compared with experimental data, as we have done in Table III. The model wavelength appears to be too short at high frequencies.

Table III. Comparison of wavelength at characteristic place

	(mm)	Frequency (KHz)
von Békésy (1960)	4.8	0.2 - 0.3
Two-dimensional model	3.8	0.4
Rhode (1971)	1.7	6.0
Two-dimensional model	0.45	6.4

The mathematical model is certainly not ready to replace experimental observation. The role of the model must remain to complement the experimental data.

8.3 Direct numerical solutions

The direct numerical solutions of the two-dimensional model equations as described in Appendix A, is reasonably accurate and has some computational advantage over previous solutions. The most accurate published solutions of the two-dimensional model are those of Allen (1977) obtained via the integral equation of section 4.1. The curves that Allen obtained are nearly identical to the curves shown in Fig. 17. Allen indicated that with 200 points representing the length of the basilar membrane, the Data General S/200 Eclipse computer required about two hours for a single solution. Our direct numerical solution for 245 points required only about 70 seconds of CPU time on a Digital Equipment Corporation PDP-10 computer. Allen's numerical scheme required storage of about 40,000 complex numbers and our scheme about 18,000 complex numbers.

Even with a 245-point solution there were some numerical errors due to an insufficient number of points. The jagged peaks at the characteristic place on the highest frequency curve in Fig. 13a and on all frequency curves in Fig. 17a are apparently due to having an insufficient number of points. This artifact also appeared in Allen's solutions. The number of points was adequate when the admittance function was not so sharply resonant.

In all the phase curves, Fig. 13b through 18b, there was an ambiguity of an integer multiple of 2π as to the total phase difference. The phase was unwrapped subject to minimum group delay. A multiple of 2π radians was added to the phase so as to minimize the absolute value of the slope of the phase. Some phase curves with steep slopes might have been unwrapped differently if more points had been taken.

This is especially true in Fig. 14b where the entire abscissa was represented by only 100 points.

8.4 The "slowly varying" approximation

The one-dimensional model is certainly less accurate than the two-dimensional model. The assumption was made that $\beta(x)$, as defined by a transcendental equation, was slowly varying. Instead, $\beta(x)$ was found to be discontinuous at the resonance of the admittance function.

In Table II the resonance of the admittance function occurs at about $x = 2.10$, where $\mathrm{Re}\left[-2i\omega\rho Y(x)H\right]$ changes from positive to negative. Note that just before the resonance place

$$\beta H \approx -2i\omega\rho Y(x)H \tag{8.1}$$

and just after the resonance place

$$\beta H \approx -i\pi/2. \tag{8.2}$$

The character of the solution changes dramatically at the resonance place. The change is also discontinuous whenever $\mathrm{Im}\left[-2i\omega\rho Y(x)H\right]$ is not zero at the resonance place.

Still, the one-dimensional model curves in Fig. 18 are quite similar to the two-dimensional model curves in Fig. 13. Comparing Fig. 18a with the Fig. 13a the agreement is quite good at low frequencies. At higher frequencies the one-dimensional model lacks the increasing slope or peaking on the stapes side of the characteristic place. In Fig. 13b the phase curves have a tendency to level-off at about 4.5π for the lowest frequencies, then there is an abrupt change to a leveling-off at 6.5π. In Fig. 18b the phase still goes to zero slope at higher

frequencies, but the point of leveling-off changes gradually. A casual comparison showed the pressure distribution in the y-direction to agree with the two-dimensional model except in the vicinity of the characteristic place.

The one-dimensional model has all the parameters of the two-dimensional model and one additional parameter, y_0, the height within the canal at which Laplace's equation would be satisfied. For the solutions in Fig. 18, y_0 was set to zero. As y_0 is increased, a peaking feature appears in the magnitude curves and the back slopes become steeper.

The most interesting and useful aspect of the one-dimensional model is the way in which the transition from "before the place" to "after the place" is embodied in the transcendental equation:

$$\beta H \tanh \beta H = -2i\omega\rho YH. \tag{8.3}$$

In a very approximate sense

$$P_d(x,0) \approx P_0 \exp\left[-i\int^x \beta(x)dx \right] . \tag{8.4}$$

In this approximation $\mathrm{Re}\left[\beta(x)\right]$ is proportional to the slope of the phase of the pressure difference and $\mathrm{Im}\left[\beta(x)\right]$ is proportional to the slope of the magnitude of the pressure. Compare the numerical values for $\beta(x)H$ found in Table II with the two-dimensional solution for the pressure difference shown in Fig. 17. Note that the slope of the magnitude is quite small until it approaches the place. At the place the slope becomes quite large very quickly and then changes abruptly to an intermediate slope. The same pattern is evident in the values of $\mathrm{Im}\left[\beta(x)H\right]$. The slope of the phase is gradually increasing from

near the stapes and becomes large near the place, but then abruptly returns to zero. The same pattern is seen in $\mathrm{Re}\left[\beta(x)H\right]$.

The "slowly varying" model is not offered as a replacement for the two-dimensional model, but as a link to other one-dimensional models based on long or short-wave approximations.

8.5 Theories of hearing

The solutions of our model for basilar membrane motion are traveling-wave solutions. As the stapes vibrates sinusoidally a wave travels down the basilar membrane. The amplitude of the wave increases gradually up to the characteristic place and then decays rapidly. One argument against a traveling-wave theory of hearing perception is that it must depend on the action of the stapes (Wever, 1949). Fig. 16 shows the basilar membrane displacement if the rigid walls of the cochlea were vibrating instead of the stapes, the shape of the traveling wave on the basilar membrane remains nearly the same for the lowest frequency. For higher frequencies the motion is still predominately a wave traveling toward the helicotrema. As the frequency is increased, the traveling wave acquires progressively more severe dips in amplitude on the stapes side of the characteristic place. Beyond the place, the basilar membrane motion is that of rigid walls with constant amplitude and phase. The steep negative slope in the magnitude of the displacement is retained at all frequencies.

The peak of the magnitude curves produced by our model is not sharp enough to explain frequency discrimination by localized motion of the basilar membrane. The steep back-slope, however, leaves room

for a place theory of frequency discrimination based on a "law of contrast." For a tone of a given frequency and loudness, there would be a sharply defined transition between places on the basilar membrane where the sensory cells were excited and places where they were not.

There is also a possible means for encoding the loudness of a tone in the basilar membrane motion. In Fig. 13a, the slope of the magnitude curves toward the stapes is consistently about 9.5 db/octave. (An octave is measured as 0.69 cm because the characteristic place will change by this distance when the frequency changes by one octave.) For a tone of a given loudness and frequency there will be a certain distance along the basilar membrane in which the sensory cells will be excited. This distance will have a linear relationship to the loudness of the tone in decibels. Further support for this mechanism of encoding loudness is given by psychoacoustic observations. According to van Bergeijk et al. (1960), an increase in the loudness level of a tone of about 9 db will double the subjective loudness. In other words, a tone which is 9 db louder sounds twice as loud. Thus, it seems that the sensation of "twice as loud" could be related to the sensation of "twice the frequency."

9. SUMMARY AND CONCLUSIONS

A two-dimensional mathematical model is developed in this thesis based on classical assumptions. The basilar membrane is represented by an acoustic admittance function with longitudinal coupling only through the cochlear fluid. The fluid is assumed to be inviscid and incompressible and all motion in the cochlea is assumed to be linear.

With these assumptions, various means are investigated for obtaining a solution to the basilar membrane motion in response to vibration of the stapes. The integral equations of Allen (1977) and Siebert (1974) are presented for the infinite cochlea and shown to be related by a Fourier transform. A two-dimensional finite difference scheme based directly on the two-dimensional model equations is presented. This direct method is as accurate as Allen's published solutions and is one-hundred times faster in computation speed. Apparently, the integral equations do not simplify matters when it comes to finding numerical solutions.

Numerical solutions are obtained by the direct method for parameters chosen primarily to fit the cochlear map. The effect of using different parameters was considered. Reducing the height of the cochlea caused the magnitude of the displacement to spread out somewhat and allowed the phase to drop further. If the stapes were assumed to be motionless and the rigid walls vibrating instead, traveling waves on the basilar membrane still moved toward the helicotrema. This is significant for a traveling-wave theory of hearing because hearing is possible through bone conduction

even when the stapes does not vibrate.

A new one-dimensional model of the cochlea is proposed which assumes the properties of the basilar membrane to vary slowly along the length of the cochlea. The numerical solutions to the one-dimensional model are nearly the same as the two-dimensional model for low frequencies. At higher frequencies the one-dimensional model lacks the increasing slope of the magnitude near the characteristic place. The transcendental equation associated with the one-dimensional model gives a relationship between the local wavelength of the basilar membrane displacement and the physical parameters of the cochlea.

Our numerical solutions are not a close fit to the experimental data obtained by Rhode. There is, however, agreement in many of the qualitative features of both the magnitude and phase curves. We should point our that although the agreement of our model with experimental data is not exact, it is considerably better than other investigators who model the basilar membrane as a beam or plate with longitudinal stiffness (Steele, 1974 and Inselberg and Chadwick, 1976). Evidently, the assumption that the basilar membrane has significant longitudinal coupling is inconsistent with experimental observation.

The magnitude curves have a 9 db/octave slope on the stapes side of the characteristic place. This slope increases as the characteristic place is approached. The magnitude falls very rapidly just beyond the place for a short distance. The magnitude then falls more gradually with a slope that is a function of the height of the cochlear canal. The initial 9 db/octave slope is, perhaps, associated with a cochlear encoding of the loudness of a tone. The steep negative back-slope

could provide a mechanism for frequency discrimination.

There is much more that could be done with this two-dimensional model. If the dimension of time were retained one could observe impulse responses with a non-linear admittance function. If the fluid were allowed to be viscous and the motion non-linear one should be able to find the "Békésy's eddies" in the fluid.

A full three-dimensional solution should be feasible using finite element techniques (Huebner, 1975). It would be valuable to know what are the effects of the circular canal and spiraling cochlea on the motion of the basilar membrane.

APPENDIX A. DESCRIPTION OF THE NUMERICAL PROCEDURE FOR THE TWO-DIMENSIONAL FINITE DIFFERENCE SCHEME

A numerical procedure will be described for obtaining solutions to the model equations developed in chapter 3. A standard, two-dimensional finite difference scheme is used to solve for $P_d(x,y)$ everywhere in the fluid (Isaacson and Keller, 1966).

Consider a two-dimensional rectangular array of points superimposed on our cochlear model. There are M points in the y-direction and N points in the x-direction. We want to solve for the pressure at these MN points. We will define

$$P(I,J) = P_d(J\,dx, I\,dx)$$

where

$$dx = L/N$$

$$I = 1, 2, \ldots, M$$

$$J = 1, 2, \ldots, N.$$

From a finite difference approximation of the model equations we have MN simultaneous algebraic equations for these unknown pressure values. The boundary conditions are incorporated into the finite-difference equations.

Let $\underline{p}$ be an MN-dimensional vector containing all the unknown pressure values. Let $\underline{q}$ be an MN-vector of initial conditions. Our finite

difference equations can be written as a matrix equation

$$A\underline{p} = \underline{q}.$$

The matrix A is a very sparse (MN) × (MN) matrix. In fact it is block-tri-diagonal, with the off-diagonal blocks being multiples of the identity matrix. We will illustrate this for the case M = N = 5.

$$\begin{pmatrix} A_1 & -2I & 0 & 0 & 0 \\ -I & A_2 & -I & 0 & 0 \\ 0 & -I & A_3 & -I & 0 \\ 0 & 0 & -I & A_4 & -I \\ 0 & 0 & 0 & -I & A_5 \end{pmatrix} \begin{pmatrix} p^1 \\ p^2 \\ p^3 \\ p^4 \\ p^5 \end{pmatrix} = \begin{pmatrix} q^1 \\ 0 \\ 0 \\ 0 \\ 0 \end{pmatrix}$$

where

$$A_K = \begin{pmatrix} a_K & -2 & 0 & 0 & 0 \\ -1 & 4 & -1 & 0 & 0 \\ 0 & -1 & 4 & -1 & 0 \\ 0 & 0 & -1 & 4 & -1 \\ 0 & 0 & 0 & -2 & 4 \end{pmatrix}$$

$$a_K = \left(4 + 2\,(2i\omega\rho Y(K\,dx) \right)$$

$$I = \begin{pmatrix} 1 & 0 & 0 & 0 & 0 \\ 0 & 1 & 0 & 0 & 0 \\ 0 & 0 & 1 & 0 & 0 \\ 0 & 0 & 0 & 1 & 0 \\ 0 & 0 & 0 & 0 & 1 \end{pmatrix}$$

$$p^K = \begin{pmatrix} P(1,K) \\ P(2,K) \\ P(3,K) \\ P(4,K) \\ P(5,K) \end{pmatrix} \qquad q^K = \begin{pmatrix} -2P_0' dx \\ -2P_0' dx \\ -2P_0' dx \\ -2P_0' dx \\ -2P_0' dx \end{pmatrix}$$

$$P_0' = 2\omega^2\rho$$

On the following pages is the Fortran code for the computer program used to obtain solutions to our two-dimensional model. Program DM3 is the main program, but most of the computation is performed in the subroutines. DM3 implements solution of the matrix equation by a Gaussian procedure for block-elimination, taking advantage of the fact that the matrix A is block tri-diagonal. The subroutines MXINT, MXINV, MXADD, and MXELM perform initializing, inverting, adding, and eliminating operations on the sub-matrices. The subroutine YBM computes the admittance of the basilar membrane at a given point, for a given frequency. DM3 is set up to solve the matrix equation with M = 8 and N = 245 for ten different frequencies and write the computed results onto the disk.

```
C  PGM:DM3
C  MAIN PROGRAM FOR 2-D COCHLEAR MODEL
       COMPLEX A(8,8,246),P(8,246),Y(246),D(246)
       COMPLEX POP,YBM,S
       REAL KO,MO
       COMMON/DATA/XL,YH,KO,RO,MO,N
       COMMON/STAPES/POP,W,RHO,DX
       DATA XL/3.5/,YH/.1/,RHO/1./
       DATA M/8/,N/245/,KO/1.E9/,RO/200./,MO/.15/
       DX=XL/FLOAT(N)
C  LOOP FOR TEN FREQUENCIES
       DO 999 IF=1,10
       FREQ=400.*1.414**(IF-1)
       W=6.2832*FREQ
       S=CMPLX(0.,W)
       POP=2.*W*W*RHO
C  INITIALIZE PRESSURE VECTOR AND MATRIX
       CALL MXINT(A,P,M,N)
C  SOLVE BLOCK MATRIX EQUATION ... WORK DOWN FROM TOP
       CALL MXINV(A,P,1,M)
       DO 10 K=2,N
       CALL MXADD(A,P,K,M)
       CALL MXINV(A,P,K,M)
10     CONTINUE
C  WORK UP FROM BOTTOM
       DO 20 K=N-1,1,-1
       CALL MXELM(A,P,K,M)
20     CONTINUE
C  COMPUTE BM DISPLACEMENT
       DO 30 I=1,N
       Y(I)=YBM(I,W)
       D(I)=Y(I)*P(1,I)/S
30     CONTINUE
C  WRITE DATA ON DISK
       WRITE(22) (P(1,I),Y(I),D(I),I=1,N)
999    CONTINUE
       END
```

```
      SUBROUTINE MXINT(A,P,M,N)
      COMPLEX A(8,8,246),P(8,246),POP,YBM,S
      COMMON/STAPES/POP,W,RHO,DX
C  INITIALIZE FIRST SUB-MATRIX AND PRESSURE VECTOR,
C    OTHERS WILL BE TAKEN CARE OF LATER.
C  THESE INITIAL VALUES ARE DIVIDED BY TWO SO THAT
C    THE FIRST INVERSE SUB-MATRIX WILL BE TIMES TWO.
      DO 10 I=1,M
      P(I,1)=-DX*POP
      DO 10 J=1,M
10    A(I,J,1)=0.
      S=CMPLX(0.,W)
      A(1,1,1)=2.+(2.*S*RHO*YBM(1,W))*DX
      A(1,2,1)=-1.
      DO 20 I=2,M-1
      A(I,I-1,1)=-.5
      A(I,I  ,1)=2.
20    A(I,I+1,1)=-.5
      A(M,M-1,1)=-1.
      A(M,M  ,1)=2.
      RETURN
      END
```

```
      SUBROUTINE MXINV(A,P,K,M)
      COMPLEX AT,A(8,8,246),P(8,246),B(8,8)
C  INVERT THE KTH SUB-MATRIX OF A(I,J,K)
C    AND SOLVE FOR THE PRESSURE.
C  WORK DOWN FROM TOP:
      DO 40 J=1,M
      IF(CABS(A(J,J,K)).LT.1.E-10)STOP
      AT=1./A(J,J,K)
      DO 10 J1=1,M
10    A(J,J1,K)=A(J,J1,K)*AT
      P(J,K)=P(J,K)*AT
      A(J,J,K)=AT
      IF(J.EQ.M)GO TO 40
      DO 30 I=J+1,M
      AT=-A(I,J,K)
      A(I,J,K)=0.
      DO 20 J1=1,M
20    A(I,J1,K)=A(I,J1,K)+A(J,J1,K)*AT
      P(I,K)=P(I,K)+P(J,K)*AT
30    CONTINUE
40    CONTINUE
C  WORK UP FROM BOTTOM:
      DO 50 I=1,M
      DO 50 J=1,I
50    B(I,J)=A(I,J,K)
      DO 60 I=1,M-1
      DO 60 J=I+1,M
60    B(I,J)=0.
      DO 80 I=M-1,1,-1
      DO 80 JI=I+1,M
      DO 70 J=1,M
70    B(I,J)=B(I,J)-A(I,JI,K)*B(JI,J)
80    P(I,K)=P(I,K)-A(I,JI,K)*P(JI,J)
C  MULTIPLY INVERSE BY -1
      DO 90 I=1,M
      DO 90 J=1,M
90    A(I,J,K)=-B(I,J)
      RETURN
      END
```

```
      SUBROUTINE MXADD(A,P,K,M)
      COMPLEX A(8,8,246),P(8,246),GAM,POP,YBM,S
      COMMON/STAPES/POP,W,RHO,DX
C  INITIALIZE THE KTH SUB-MATRIX AND
C    ADD THE PREVIOUSLY INVERTED (K-1)TH SUB-MATRIX.
C         LET A(K)=A(K)+A(K-1)
C         LET P(K)=P(K)+P(K-1)
C
      KM=K-1
      DO 10 I=1,M
      P(I,K)=P(I,KM)
      DO 10 J=1,M
10    A(I,J,K)=A(I,J,KM)
      S=CMPLX(0.,W)
      A(1,1,K)=A(1,1,KM)+4.+2.*(2.*S*RHO*YBM(K,W))*DX
      A(1,2,K)=A(1,2,KM)-2.
      DO 20 I=2,M-1
      A(I,I-1,K)=A(I,I-1,KM)-1.
      A(I,I  ,K)=A(I,I  ,KM)+4.
20    A(I,I+1,K)=A(I,I+1,KM)-1.
      A(M,M-1,K)=A(M,M-1,KM)-2.
      A(M,M  ,K)=A(M,M  ,KM)+4.
      RETURN
      END
```

.....

```
      SUBROUTINE MXELM(A,P,K,M)
      COMPLEX A(8,8,246),P(8,246),AP
C  ELIMINATE THE UPPER-DIAGONAL SUB-MATRICES
C         LET P(K)=P(K)-A(K)*P(K+1)
C
      DO 20 I=1,M
      AP=0.
      DO 10 J=1,M
10    AP=AP+A(I,J,K)*P(J,K+1)
      P(I,K)=P(I,K)-AP
20    CONTINUE
      RETURN
      END
```

```
      COMPLEX FUNCTION YBM(I,W)
      REAL K,M,KO,MO
      COMPLEX S
      COMMON/DATA/XL,YH,KO,RO,MO,NPTS
C  COMPUTE BASILAR MEMBRANE ADMITTANCE
      S=CMPLX(0.,W)
      X=XL*FLOAT(I-1)/FLOAT(NPTS)
      AX=X
      K=KO*EXP(-2.*AX)
      R=RO
      M=MO
      YBM=1./(K/S+R+M*S)
      RETURN
      END
```

APPENDIX B. SOLVING THE TRANSCENDENTAL EQUATION BY ITERATION

An algorithm is needed to solve the equation

$$x = y \tanh(y)$$

for y, given x and an initial guess for y. Both x and y are complex numbers, The equation is solved by Newton iteration (Isaacson and Keller, 1966). Consider the function f(y) defined by

$$f(y) = x - y \tanh(y).$$

The problem is to find y such that f(y) = 0. Given an initial guess y_0, the iteration scheme makes successive improvements in the initial guess, y_i, by the rule

$$y_{i+1} = y_i - \frac{f(y_i)}{f'(y_i)} .$$

With some manipulation this becomes

$$y_{i+1} = \frac{y_i^2 + x \cosh(y_i)}{y_i + \sinh(y_i) \cosh(y_i)} .$$

Iteration is terminated when

$$f(y) < \varepsilon |x|$$

where ε is some small number.

A Fortran subroutine named ATNH implements the above algorithm and is given on the following page. The subroutine will make its own initial guess for extreme values of x. This subroutine is used by our "slowly varying" model. The initial guess supplied to the subroutine is always the previously returned value.

```
      SUBROUTINE ATNH(X,Y)
C  SOLVES EQUATION X=Y*TANH(Y)
C   FOR Y, GIVEN X AND AN INITIAL GUESS FOR Y.
      COMPLEX X,Y,T,EX,S,C
      PID2=1.570796327
      EPS=1.E-4
C  CHECK IF ABS(X) IS SMALL
      XM=CABS(X)
      IF(XM.LT..1)Y=-CSQRT(X)
      IF(XM.LT..01)RETURN
C  CHECK IF REAL(X) IS LARGE
      XR=REAL(X)
      IF(XR.GT.2.)Y=X
      IF(XR.GT.30.)RETURN
C  CHECK FOR REAL(X) NEGATIVE
      IF(XR.LT.0.)Y=CMPLX(0.03,-1.5)
C  START NEWTON ITERATION FOR Y
      DO 10 I=1,100
      YI=AIMAG(Y)
      IF(YI.GT.0.)Y=-Y
      IF(YI.LT.-PID2.AND.XR.LT.0.)Y=CMPLX(0.03,-1.5)
      EX=CEXP(Y)
      S=(EX-1./EX)/2.
      C=(EX+1./EX)/2.
      Y=(Y*Y+X*C*C)/(Y+S*C)
      T=Y*S/C
      IF(CABS(1.-T/X).LT.EPS)RETURN
10    CONTINUE
C  ITERATION FAILED TO CONVERGE
      TYPE 20,X,Y,T
20    FORMAT(' %ATNH:X='1P2E9.2'  Y='1P2E9.2'  T='1P2E9.2)
      RETURN
      END
```

REFERENCES

Allaire, P., Raynor, S., and Billone, M. (1974). "Cochlea Partition Stiffness-A Composite Beam Model," J. Acoust. Soc. Am. 55, 1252-1258.

Allen, J. B. (1977). "Two-Dimensional Cochlear Fluid Model: New Results," J. Acoust. Soc. Am. 61, 110-119.

von Békésy, G. (1960). Experiments in Hearing (McGraw-Hill, New York).

van Bergeijk, W. A., Pierce, J. R., and David, E. E. (1960). Waves and the Ear (Doubleday, Garden City, New York).

Chadwick, R. S., Inselberg, A., and Johnson, K. (1976). "Mathematical Model of the Cochlea. II: Results and Conclusions," SIAM J. Appl. Math. 30, 164-179.

Flanagan, J. L. (1972). Speech Analysis Synthesis and Perception (Springer-Verlag, New York).

Gradshteyn, I. S. and Ryzhik, I. M. (1965). Table of Integrals, Series, and Products (Academic Press, New York).

Hall, J. L. (1974). "Two-Tone Distortion Products in a Non-Linear Model of the Basilar Membrane," J. Acoust. Soc. Am. 56, 1818-1828.

Helmholtz, H. L. (1954). On the Sensations of Tone (Dover, New York).

Huebner, K. H. (1975). The Finite Element Method for Engineers (Wiley, New York).

Inselberg, A. and Chadwick, R. S. (1976). "Mathematical Model of the Cochlea. I: Formulation and Solutions," SIAM J. Appl. Math. 30, 149-163.

Isaacson, E. and Keller, H. B. (1966). Analysis of Numerical Methods (Wiley, New York).

Johnstone, B. M. and Boyle, A. J. F. (1967). "Basilar Membrane Vibrations Examined with the Mössbauer Technique," Science 158, 389-390.

Kim, D. O., Molnar, C. E., and Pfeiffer, R. R. (1973). "A System of Non-Linear Differential Equations Modeling Basilar Membrane Motion," J. Acoust. Soc. Am. 54, 1517-1529.

Kim, D. O. and Molnar, C. E. (1975). "Cochlear Mechanics: Measurements and Models," in Nervous System, B. Tower, Editor-in-Chief, Vol. 3: Human Communication and Its Disorders (Raven Press, New York).

Lesser, M. B. and Berkley, D. A. (1972). "Fluid Mechanics of the Cochlea. Part 1," J. Fluid Mech. 51, part 3, 497-512.

Lien, M. D. and Cox, J. R. (1973). "A Mathematical Model of the Mechanics of the Cochlea," Ph.D. dissertation (Sever Institute of Washington University, St. Louis, MO) (unpublished).

Novoselova, S. M. (1975). "The Basilar Membrane as an Elastic Plate," Sov. Phys. Acoust. 21, 56-60.

Peterson, L. C. and Bogert, B. P. (1950). "A Dynamical Theory of the Cochlea," J. Acoust. Soc. Am. 22, 369-381.

Ranke, O. F. (1950). "Theory of Operation of the Cochlea: A Contribution to the Hydrodynamics of the Cochlea," J. Acoust. Soc. Am. 22, 772-777.

Rhode, W. S. (1971). "Observations of the Vibration of the Basilar Membrane Using the Mössbauer Technique," J. Acoust. Soc. Am. 49, 1218-123i.

Rhode, W. S. and Robles, L. (1974). "Evidence from Mössbauer Experiments for Non-Linear Vibration in the Cochlea," J. Acoust. Soc. Am. 55, 588-596.

Schroeder, M. R. (1973). "An Integrable Model for the Basilar Membrane," J. Acoust. Soc. Am. 53, 429-434.

Schroeder, M. R. (1975). "Models of Hearing," Proc. IEEE 63, 1331-1350.

Siebert, W. A. (1974). "Ranke Revisited-A Simple Short-Wave Cochlea Model," J. Acoust. Soc. Am. 56, 148-162.

Sondhi, M. M. (1977). "A Method for Computing Motion in a Two-Dimensional Cochlear Model," (Bell Laboratories, Murray Hill, NJ) (unpublished).

Steele, C. R. (1974). "Behavior of the Basilar Membrane with Pure Tone Excitation," J. Acoust. Soc. Am. 55, 148-162.

Weinberger, H. F. (1965). Partial Differential Equations (Xerox College Pub., Lexington, MA).

Wever, E. G. (1949). Theory of Hearing (Wiley, New York).

Wever, E. G. and Lawrence, M. (1954). Physiological Acoustics (Princeton University Press, Princeton, New Jersey).

Zweig, G., Lipes, R., and Pierce, J. R. (1976). "The Cochlear Compromise," J. Acoust. Soc. Am. 59, 975-982.

Zwicker, E. and Terhardt, E. (ed.) (1974). Facts and Models in Hearing (Springer-Verlag, New York).

Zwislocki, J. J. (1965). "Analysis of Some Auditory Characteristics," Handbook of Mathematical Psychology, Luce, R. D., Bush, R. R., and Galanter, E., Eds. (Wiley, New York), Vol. 3, pp. 1-98.